RSC Advances

REVIEW

Check for updates

Cite this: *RSC Adv.*, 2024, **14**, 9445

Exploring microgel adsorption: synthesis, classification, and pollutant removal dynamics

Muhammad Arif *

Microgels have gained significant importance for the removal of pollutants owing to their stimulus-responsive behavior, high stability, and reusable capacity. However, despite these advantages, several hurdles need to be overcome to fully maximize their potential as effective adsorbents for eradicating various contaminants from the environment, such as metallic cations, organic compounds, anions, harmful gases, and dyes. Therefore, a critical review on the adsorption of pollutants by microgels is needed. In this regard, this review presents the latest developments in the adsorptive properties of microgels. The synthetic methods, architectural structures, and stimulus-responsive behavior of microgels are explained in detail. In addition, this review explores various factors that directly influence the adsorption of pollutants by microgels, such as pH, feed composition, content of pollutants, content of comonomers, agitation time, temperature, microgel dose, nature of both adsorbates (pollutants) and adsorbents (microgels), nature of the medium, and ionic strength. Various adsorption isotherms are also explored together with the kinetic aspects of the adsorption process to provide a comprehensive understanding.

Received 22nd January 2024
Accepted 7th March 2024

DOI: 10.1039/d4ra00563e

rsc.li/rsc-advances

1. Introduction

The environment is affected by a variety of organic,[1] inorganic,[2] and biological[3] pollutants introduced through both artificial and natural processes. Inorganic pollutants include a variety of noxious heavy metal cations[4] and anions.[5] The presence of these ions in wastewater is detrimental to aquatic life. Furthermore, wastewater contains diverse organic substances such as toxic dyes,[6] herbicides,[7] antibiotics,[8] and aromatic compounds.[9] A portion of these contaminants has the potential to accumulate in the environment and become integrated into the food chain, affecting living organisms. Furthermore, heavy metals can inflict harm upon living organisms considering their reactivity with organic species.

Thus, numerous methods have been devised for the treatment of water containing various pollutants. These methodologies include flocculation,[10] cementation,[11] coagulation,[12] evaporation,[13] electrocoagulation,[14] ion exchange,[15] membrane filtration,[16] and adsorption.[17] However, these techniques are associated with certain limitations, notably their high cost and the challenge of managing sludge disposal following wastewater treatment. Among the above-mentioned methods, adsorption stands out because of its numerous advantages in wastewater treatment, including its high removal efficiency, cost-effectiveness with its reuse, ease of use, and wide array of available adsorbents. Thus, the primary goal of recent research has been to innovate and create novel adsorbents for effectively remediating contaminated water.

Among the various adsorbent options,[18–21] microgels (three-dimensional crosslinked network of organic polymers) are highly favored because of their responsive nature and customizable properties.[22–24] The ease of preparation,[25] substantial adsorption capacity,[26] long-term stability,[27] impressive mechanical resilience,[28] and reusability[29] of microgels make them exceptionally effective for the removal of pollutants from wastewater. Additionally, microgels offer the versatility of incorporating different functional groups into their network, such as sulphonic,[30] amide,[31] carbonyl,[32] hydroxyl,[33] carboxylic,[34] and amine[35] groups, thereby functioning as chelating agents to extract pollutants from aqueous solutions. These functional groups also impart pH and ionic strength sensitivity to the microgel. The most commonly employed comonomers for polymerizing microgel adsorbents to induce multi-sensitivity and chelating properties are acrylic acid,[36] ethyleneimine, acrylamide,[35] 2-acrylamido-2-methylpropane sulfonic acid,[30] and vinyl imidazole.[37] Acrylic acid (AAc) has a pK_a value of 4.25, which means that when the pH exceeds its pK_a, poly(*N*-isopropylacrylamide-AAc) P(NIPr-AAc) copolymer microgels swell due to the deprotonation of the carboxylic acid groups of AAc, as reported by Picard *et al.*[38] The substantial negative charge present within microgels renders them highly effective as adsorbents for extracting heavy metal ions[39–42] as well as various dyes[43–49] from aqueous solutions. Additionally, positively charged microgels can be employed as efficient

Department of Chemistry, School of Science, University of Management and Technology, Lahore 54770, Pakistan. E-mail: Muhammadarif2861@yahoo.com; Muhammadarif@umt.edu.pk

This article is licensed under a Creative Commons Attribution-NonCommercial 3.0 Unported Licence.

© 2024 The Author(s). Published by the Royal Society of Chemistry

adsorbents for capturing negatively charged pollutants.[50–54] Hence, the adsorption capacity of P(NIPr)-based microgels can be enhanced with introduction of diverse functional groups in their structure[55–57] from aqueous solution. Moreover, the pollutant uptake capacity of microgels can be adjusted by altering the pH[36] and temperature[57] of the medium due to their sensitivity to pH, temperature, and their volume phase transition characteristics. A review on the adsorption of pollutants by microgels was reported in 2018 by Naseem *et al.*,[58] but since then, numerous studies been reported on adsorption by microgels. According to Scopus data, 2471 articles have been reported on microgels from 2018 to date. Among these articles, 208 are related to the adsorption of pollutants by microgels. These articles provided different information related to the removal of pollutants by microgels.

Maintaining control of the polydispersity of microgel particles and the dimensions and shapes of microgels, attracting the pollutants from wastewater through the polymeric network, increasing the adsorption capacity of microgels, addressing the aggregation of microgels under different solvents or during the adsorption of pollutants, and releasing the adsorbed pollutant to enable the reuse of microgels have all presented persistent challenges in this field. Thus, over the past a few years, significant efforts have been dedicated to achieving microgels with high mono-dispersity, precise control of their shape and size, outstanding stability, and efficient recoverability. In this case, a review is required to provide all the latest information to researchers. To the best of our knowledge, there are no comprehensive reviews summarizing the advancements in the adsorptive property of microgels over the past few years.

2. Adsorptive pollutant removal by microgels (adsorbents)

According to Scopus data, 124 491 articles have been published on environmental pollutants from 2018 to present. This quantity indicates that the amount of pollutants in the environment is rapidly increasing, which can be divided into various types of pollutants and removed from the environment by microgels through the adsorption process.

The global concern over organic dye and heavy metal cation contamination in the aquatic environment has arisen due to the introduction of a significant volume of these pollutants from various sources. This type of pollution from the release of water containing dyes and heavy metals is attributed to the rapid industrialization such as leather tanning,[59] textiles,[60] battery manufacturing,[61] electroplating,[62] and food additives.[63] The commonly found heavy metals in wastewater include arsenic (As), copper (Cu), cadmium (Cd), lead (Pb), mercury (Hg), nickel (Ni), zinc (Zn), manganese (Mn), chromium (Cr), and cobalt (Co), which are present in different oxidation states. Dye-[64] and heavy metal[65]-contaminated water poses a significant threat to the well-being of living organisms. Toxic heavy metals such as arsenic (As) enter water sources through various means. Arsenic is particularly problematic given that it is a persistent pollutant in both underground and drinking water and known for its highly carcinogenic properties.[66] The contamination of water with arsenic is primarily attributed to biological activities and geochemical reactions, and its presence in the Earth's crust further contributes to its occurrence in water. The World Health Organization has established the maximum allowable concentration of arsenic in drinking water at 10 $\mu g\ L^{-1}$.[67] Prolonged exposure to arsenic can lead to health issues including skin cancer, anorexia, anemia, and various malignancies in humans. Also, although copper (Cu) is an essential element for human health,[68] excessive levels of copper in the body can result in poisoning and severe symptoms such as diarrhea, vomiting, and abdominal pain. Copper (Cu) accumulation in the human body can also lead to damage in the kidneys and liver, potentially resulting in gastrointestinal ulcers, shock, and even fatality. Lead (Pb) in water can pose severe health risks, particularly affecting pregnant women and children.[69] Similar to copper, lead can harm the kidneys and liver and cause muscular paralysis, growing issues, and in extreme cases, death in humans. Regarding dyes, it is noteworthy that only 30% of dyes used in the textile industry is classified as reactive, while the remaining 70% finds its way into the environment through textile and industrial wastewater. Dyes containing anthraquinone, oxazine, and azo functional groups are particularly reactive and contribute to environmental contamination.[70] The complicated aromatic molecular structure of synthetic dyes results in their significant structural diversity, making them highly toxic. In many developing nations, the presence of azo dyes in wastewater has emerged as a significant issue.[71] Organic dyes possess mutagenic, poisonous, and carcinogenic properties. Due to their elevated toxicity and accompanying risks, heavy metals and dyes present a significant danger to both the well-being of humans and the aquatic environment. The effective extraction of toxic dyes[72] and heavy metals[42] from water can be achieved through the use of microgel suspensions as adsorbents, which showed remarkable efficiency in pollutant removal. Some of the most frequently removed dyes from aqueous solutions using microgel adsorbents include rhodamine-B (RB),[72] methylene blue (MBl),[73] Eosin Y (EY),[74] Congo red (CRe),[75] malachite green (MGr),[76] and methyl orange (MOr).[77] Arif *et al.*[78] employed hydrogels composed of poly(-styrene)@poly(*N*-isopropylmethacrylamide) P(St)@P(NIPMe) microgel system as an adsorbent for the extraction of Cu^{2+} ions from aqueous solutions. They also converted the loaded copper(II) ions into copper nanoparticles, and then used the synthesized system as a catalyst for the reduction of different pollutants from water. Xu *et al.*[79] utilized poly(*N*-isopropylacrylamide-vinyl imidazole) P(NIPr-VIDa) microgels as an adsorbent for removing Cu^{2+} ions from aqueous environments. They also examined the effect of temperature on the adsorption capacity of the microgels. Meanwhile, Işıkver *et al.*[80] developed a microgel system that had both acid and basic groups in its structure and these groups enhanced the adsorption capacity. By replacing each reactive site with two amidoxime functional groups, the carboxylic groups, in anionic form, attract the cationic pollutants and the amino groups of microgels, in cationic form, attract the anionic pollutants due to opposite charge interactions. These types of microgels are the

© 2024 The Author(s). Published by the Royal Society of Chemistry

best materials for adsorption due to their ability to remove all types of pollutants (cationic, neutral, and anionic pollutants). These types of microgels form hydrogen bonding or ion–diploe interactions with pollutants. These types of interactions are the strongest among the interactions. Naseem *et al.*[81] utilized P(NIPMe-AAc) microgels as an adsorbent for both cationic and anionic dyes from water. At high pH and low temperature, the microgels adsorbed a greater amount of cationic dyes compared to anionic dyes due to their carboxylate ions. Alternatively, at high temperature, the microgel adsorbed more of CRe due to its dominant hydrophobic nature.

Carbon dioxide is also present in the environment. In this molecule, the carbon atom is bonded with two oxygen atoms by double bonds. The electronegativity of oxygen atoms is greater than carbon. Therefore, the carbon atom of CO_2 can get electronic cloud from another electron-donating species according to the Lewis acid–base theory. The carbon dioxide molecules act as an acid and the adsorbent species as a base. Species with greater electron-donating capacity than oxygen are responsive to their type of phenomenon. Molecules that have nitrogen or oxygen (in neutral or anionic form) in their structure are more suitable for this purpose. Therefore, these types of adsorbents that have nitrogen atoms in their structure are applied for the adsorption of CO_2 gas. For example, Yao *et al.*[82] reported the synthesis of microgels with both nitrogen and oxygen atoms in their structure, which were used for the adsorption of CO_2. A large amount of CO_2 gas was adsorbed on the surface of the microgels due to their high porosity and presence of both nitrogen and oxygen atoms as electron-pair donor sites in the structure of the microgels. Similarly, Avais and coworkers[83] synthesized a nitrogen atom-containing microgel system and used it for CO_2 adsorption. They also used this system for the adsorption of other pollutants such as MOr, MBl, nitrogen, methane, and iodine. The adsorption of CO_2 increases with an increase in the porosity of microgels, as reported by Ghani *et al.*[84] The porosity of microgels can be increased or decreased by the addition of fly ash (SiO_2, Al_2O_3, Fe_2O_3, CaO, MgO, C, K_2O, SO_3 and others). Therefore, CO_2 adsorption can also be controlled by the introduction of fly ash. Qiu *et al.*[85] synthesized a microgel and used it for adsorption of CO_2 in the presence and absence of insect-inspired coordination. Microgels are the most suitable adsorbents for the adsorption of CO_2 together with other pollutants due to their high porosity and presence of electron-pair donor sites in their structures.

Some other pollutants such as uranium,[86] phosphate,[37] dichromate, arsenate,[87] and permanganate[88] ions, as well as various aromatic compounds such as bisphenols (bisphenol F (BPF), bisphenol E (BPE), bisphenol B (BPB) and bisphenol A (BPA)),[89] anthocyanins,[90] naphthalene and 1-naphthylamine,[91] and surfactants[92] can be effectively eliminated from aqueous solutions using different types of microgel adsorbents. Hydrogen,[93] methane,[83] and iodine[94] can also be separated by microgels through adsorption. Phenols and their related compounds are widely recognized as environmental pollutants, originating from their application in the manufacturing of diverse substances such as preservatives, bactericides, pesticides, and pharmaceuticals.[95] Refineries and various petrochemical processes generate substantial wastewater containing phenolic pollutants, which pose a significant carcinogenic risk to humans. Uranium, which is known for its extreme toxicity, radioactivity, and carcinogenic properties, can lead to numerous health problems in humans.[96] Phosphate ions are used as fertilizers, but these ions are highly toxic.[97] They are extensively used in agriculture and can be fatal when ingested at elevated quantities, whether accidently or intentionally. Avais *et al.*[83] synthesized a poly(diamine) P(DAm)-based microgel and applied it as an adsorbent to extract various pollutants from the environment. Kubiak *et al.*[89] synthesized a microgel system and used it for the adsorption of bisphenol in a mixture of two different solvents (water and methanol). The extraction of bisphenol increased with an increase in the percentage of methanol. As the percentage of methanol increased, the swelling of the microgel increased. Therefore, greater adsorption occurred with an increase in the percentage of methanol.

3. Synthesis of microgels (adsorbents)

Microgels employed as adsorbents can be produced using the following techniques.

3.1. By irradiation

Microgels can be synthesized through irradiation by combining various monomers and comonomers in the absence[98] of a crosslinker followed by exposure to radiation for a specific duration. This process triggers polymerization, leading to the formation of microgels. Irradiation induces crosslinking in the structure of polymers to form microgels. The irradiation approach is favored over certain chemical methods for microgel preparation. Particular hydrogels and microgels are chosen due to concerns regarding the toxicity of chemical crosslinking agents, which can react with the functional groups on microgel particles, potentially reducing their quantity and subsequently diminishing their adsorption capability for various pollutants. Consequently, the irradiation process yields a product with high purity. In the work conducted by Matusiak *et al.*,[99] poly(acrylic acid) P(AAc) microgels with varying linear poly(acrylic acid) contents were crafted using the irradiation method, as shown in Fig. 1, with an electron beam serving as the source of irradiation. To synthesize the microgel, a predetermined quantity of AAc was used to prepare linear P(AAc) by heating their aqueous solution at 50 °C for 12 h. Then, different concentrated (10.0 mmol dm^{-3}–25 mmol dm^{-3}) solutions of linear P(AAc) were prepared and irradiated at pH 2.0 to form microgels. The radiation converted the linear polymer systems into crosslinked polymer through radical polymerization method. Irradiation triggered both crosslinking and degradation reactions simultaneously, leading to the creation of microgel particles. The radiation parameters used during synthesis are as follows: electron energy = 6 MeV, pulse frequency = 0.5 Hz, pulse duration = 2 μs, and ionizing radiation absorbed dose per single pulse = 0.9 kGy. A higher concentration of polymers also increased the crosslinking density of the microgels due to the longer distance of coils and lower number of radicals per chain.

© 2024 The Author(s). Published by the Royal Society of Chemistry

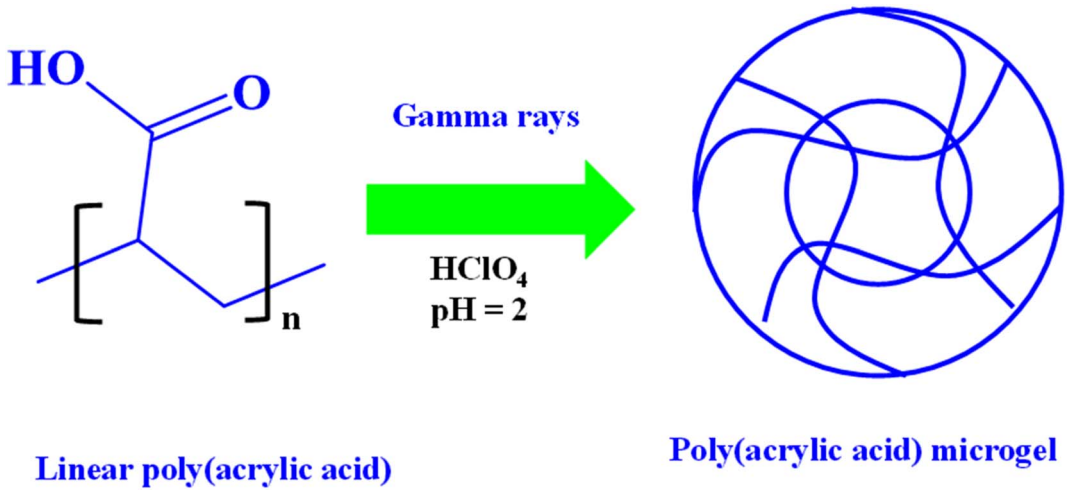

Fig. 1 Schematic diagram showing the synthesis of poly(acrylic acid) P(AAc) microgels from linear pol(acrylic acid) P(AAc) using the irradiation method.[99]

Consequently, a higher degree of microgel formation was achieved at a higher concentration of linear polymer. Cruz *et al.*[100] also synthesized microgels based on irradiation. Chitosan-based microgels were synthesized first, which were then mixed with *N*-vinyl caprolactam (NVCa) in acetic acid and radiated using a ^{60}Co gamma source. The resulting microgels were extracted with acetic acid to remove the monomers, and then water to remove acetic acid for purification.

3.2. By emulsion polymerization

Microgels can also be fabricated through the process of emulsion polymerization, which is the most commonly employed technique by researchers for producing microgel particles. In this approach, a mixture containing monomers, crosslinkers, surfactants, comonomers, and initiators is combined in deionized water. This mixture is continuously stirred, purged with nitrogen, and heated at temperatures equal to or greater than 70 °C for a duration of 4 h. After synthesis, the microgels are subjected to dialysis to eliminate any unreacted components.

Rahman *et al.*[76] also synthesized poly(methacrylic acid) P(MAAc) microgels using methacrylic acid (monomer) and *N*,*N*′-methylenebisacrylamide (MBAc) (crosslinker). Span 80 and cyclohexane were poured into a round-bottom flask and heated at 40 °C with continuous stirring. After 15 min, methacrylic acid (MAAc) (monomer), MBAc (crosslinker), ammonium persulfate (APSu) (free radical initiator), and *N*,*N*,*N*′,*N*′–tetramethylethylenediamine (accelerator) were put into the reaction flask and the reaction continued for 4 h under nitrogen and the same temperature (40 °C). The product was filtered and washed with acetone and water, and then neutralized with NaOH (1 mM) solution. The synthesized microgel was used as an adsorbent for malachite green and methylene blue. These microgels possessed a high adsorption capacity due to the opposite charges on the adsorbate (cationic dye) and adsorbent (anionic microgel) at pH 5.5. In the study conducted by Shahid *et al.*,[101] poly(*N*-isopropylacrylamide-acrylamide-methacrylic acid) P(NIPr-AAm-MAAc) copolymer microgels were manufactured using the emulsion polymerization method, and subsequently these particles were utilized as an adsorbent for the removal of Co^{2+} ions from an aqueous solution. Then, the loaded Co^{2+} ions were reduced into cobalt nanoparticles by an *in situ* reduction method, as shown in Fig. 2. NIPr (monomer), AAm and MAAc (comonomers), MBAc (crosslinker), and sodium dodecyl sulfate (SDSu) (surfactant) were mixed and added to a round-bottom flask containing water and stirred under nitrogen. The temperature of reaction increased up to 70 °C and 5 mL of ammonium per sulphate (radical initiator) was poured dropwise under nitrogen. The reaction proceeded for a further 4 h to complete polymerization. The appearance of a milky color indicated the formation of microgels. Then, the product was dialyzed to remove the unreacted moieties. During this process, SDSu was used to control the size of the particles. Subsequently, the synthesized microgels were used to adsorb Co^{2+} ions from aqueous medium under different conditions for optimization of the process. The adsorbed Co^{2+} ions were reduced to generate Co nanoparticles, and then used for catalytic purposes. Numerous other scientists have successfully generated a range of microgel suspensions with specific attributes using this approach, as demonstrated by previous studies.

3.2.1. Seed-mediated emulsion polymerization. Core-shell microgels (microgels in which one material is encapsulated in crosslinked organic polymer) can also be produced through a two-step seed-mediated emulsion polymerization technique. This approach involves first preparing polymer seeds of one type, which are subsequently utilized as the central core for the encapsulation of another type of polymer shell around them. In one of our studies,[102] a core–shell microgel with a polystyrene P(St) core and a temperature-responsive poly(*N*-isopropylmethacrylamide) P(NIPMe) shell was prepared using the seed-mediated emulsion polymerization method, as shown in Fig. 3. Initially, a Pt core was synthesized by employing styrene (St) as the monomer, NIPMe as the polarity inducer, sodium dodecyl sulfate (SDSu) as the surfactant and APSu as the free

© 2024 The Author(s). Published by the Royal Society of Chemistry

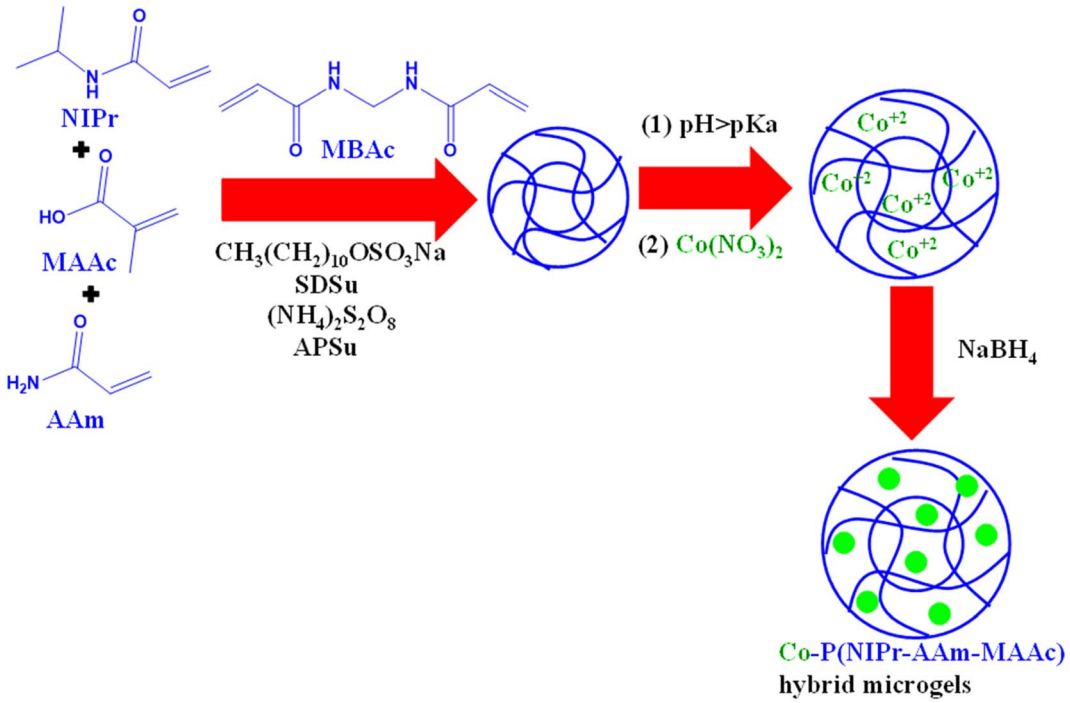

Fig. 2 Schematic showing the synthesis of cobalt nanoparticle-loaded P(NIPr-AAm-MAAc) hybrid microgels.[101]

radical initiator. This core formation process took place at 80 °C, with continuous nitrogen supply and stirring, and nucleation was accomplished within 7 h. In the subsequent stage, the P(NIPMe) shell was produced around the P(St) core using the conventional emulsion polymerization technique. Naseem *et al.*[103] similarly fabricated core–shell microgel particles composed of a P(St) core and P(NIPMe-AAc) shell using this approach. These core–shell microgels were also effectively employed as adsorbents for eliminating contaminants from aqueous solutions.

4. Classifications

Incorporating different polymeric/nonpolymeric materials in the structure of microgels enhances both their adsorptive characteristics and regenerative capacity after the adsorption of pollutants. These adsorbents can be categorized based on the morphology of various polymeric/nonpolymeric materials along the structure of the microgels, as shown in Fig. 4.

4.1. Simple microgels

Simple microgels consist only of monomer with[104] or without[105] commoners. The addition of comonomers helps to enhance their adsorption capacity or induce stimulus-responsive behavior, which supports the selective and greater adsorptive property of microgels. For example, Ghasemi *et al.*[106] synthesized a P(NIPr)-based microgel and used it for the adsorption of copper(II) ions from water. The synthesized microgels adsorb copper(II) ions due to the presence of polar amide groups in their structure. Due to this polar structure, microgels can

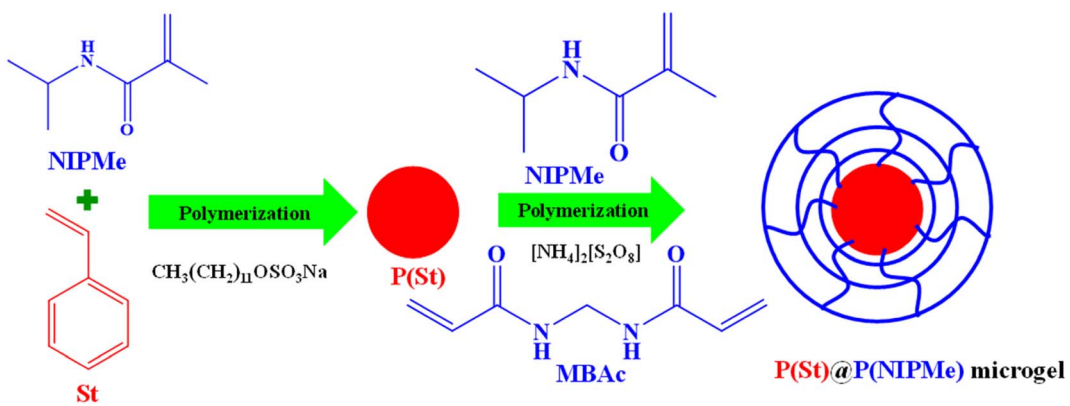

Fig. 3 Schematic showing the synthesis of P(St)-encapsulated P(NIPMe) microgels.[102]

© 2024 The Author(s). Published by the Royal Society of Chemistry

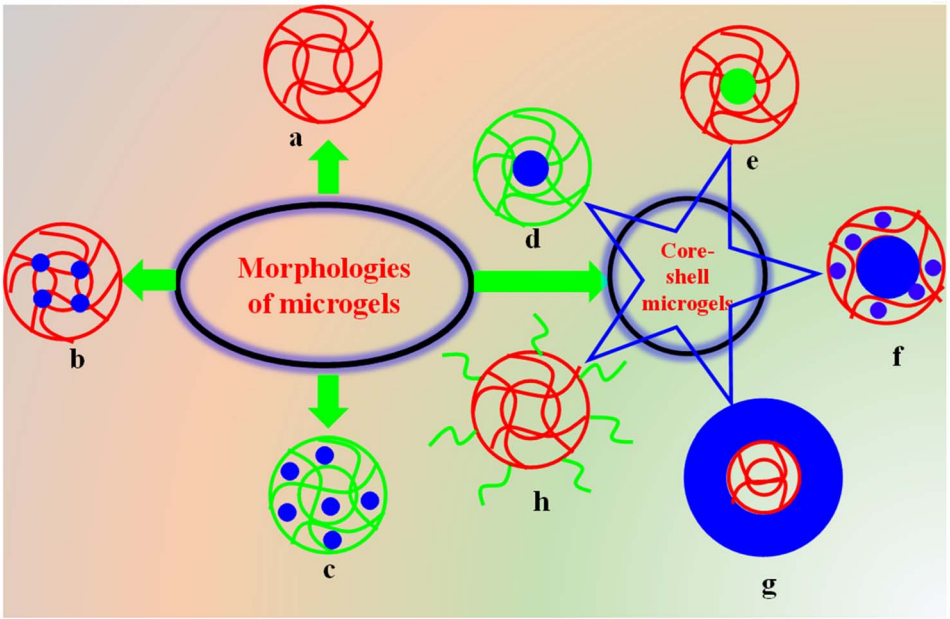

Fig. 4 Morphologies of (colors: red and green color = organic polymer material, blue = inorganic materials or metal ions) (a) simple microgels, (b) Fe_3O_4-crosslinked organic polymer microgels, (c) homogenous inorganic–organic microgel composites, (d) inorganic core encapsulated with organic polymer shell, (e) organic core encapsulated with organic shell, (f) inorganic core encapsulated with organic shell, (g) organic core encapsulated with inorganic shell, and (h) organic core encapsulated with linear organic polymer shell.

adsorb both cationic and anionic pollutants. Selectivity in microgels can be induced by adding comonomers during the synthesis. These comonomers are pH sensitive and convert the structure of microgels in anionic or cationic form by varying the pH of the medium. This induction produces selectivity for the adsorption of pollutants together with swelling/de-swelling behavior as well as electrostatic interactions. Cationic microgels repel cationic pollutants due to their same charges, whereas they attract anionic pollutants. Alternatively, anionic microgels repel anionic pollutants and attract cationic pollutants. For example, Pany *et al.*[32] used acrylic acid as a comonomer together with NIPr monomer to synthesize a microgel system. This microgel system was converted into pH-responsive systems due to the introduction of comonomer (AAc). At pH $\geq$ pK_a of AAc, the microgel was present in anionic form. Thus, the microgel adsorbed the maximum number of cationic pollutants due to its anionic structure and swelling state. Yang *et al.*[37] reported the adsorption capacity of a cationic microgel system. Kyrey *et al.*[107] and Naseem *et al.*[81] also reported the preparation of microgels with and without comonomers, respectively, and their use as adsorbents for the removal of toxic pollutants.

Simple microgels are widely reported in the literature due to their easy synthetic approach. The regeneration of these microgels after the adsorption of pollutants requires ultra-fast centrifugation due to their low density. Therefore, some amount of adsorbed pollutant comes out from the crosslinked network system, which is the only drawback of these systems.

4.2. Core–shell microgels

In core–shell microgels, two types of regions are present in their morphology, where one is the core and other is the shell. The core can be made with organic or inorganic materials, and similarly the shell regions can also be made up of organic or inorganic materials. Due to the material present in the core and shell region of microgels, these systems can be further divided into different classes.

4.2.1. Inorganic core encapsulated with organic polymer shell. In inorganic core encapsulated with organic polymer shell systems, their core region is made up of inorganic materials (SiO_2, Fe_2O_3 or Fe_3O_4) and their shell region with organic crosslinked polymers. They are very effective with respect to adsorptive properties. The density of these core–shell microgels are greater than simple microgels. Therefore, these types of microgels can easily be recycled by simple centrifugation. If the core region of core–shell systems is made with Fe_3O_4, which is paramagnetic in nature, they can be very easily recycled by applying an external magnetic field. However, a drawback of these systems is their decreased stimulus-responsive behavior, as reported in my pervious review article[108] and deformation in the shape of the microgels.[109] Al-Hussaini *et al.*[110] reported the preparation of an Fe_2O_3 core encapsulated with organic polymer with a nearly spherical-like shape. Wi *et al.*[111] also reported the synthesis of a core–shell microgel system, in which Fe–amino-clay–Fe_2O_3 was the core and poly(vinyl alcohol) P(VAl) was the shell. The synthesized core–shell microgel showed selective adsorption for anionic dyes due its cationic structure at low pH value. At low pH, the microgel structure is present in the swollen state due to the electrostatic repulsion by the same charges. The adsorption capacity of the microgel increased due to the opposite charges on both the adsorbent and adsorbent. This type of system is very important due to its selective adsorption and easily reusable properties.

© 2024 The Author(s). Published by the Royal Society of Chemistry

This class of microgels is very important for adsorption, which is due to their easily recyclable property and minimum release of adsorbed pollutants from the crosslinked network of the microgels during recycling.

4.2.2. Organic core encapsulated with organic polymer shell. In organic core encapsulated with organic polymer shell systems, their core is made up of an organic material, and their shell region also made up of organic polymers. The density of these core–shell systems is greater than homogenous microgels but less than core–shell systems in which an inorganic core is encapsulated be an organic polymer. Therefore, their recycling after adsorption is intermediate between the previously discussed systems. Me and my coworkers[102] reported the synthesis of a P(St) core encapsulated with P(NIPMe) shell to form core–shell microgels. The synthesized system was used for the adsorption of copper(II) ions. The adsorption capacity of this system was 71.94 mg g^{-1}, which was very low. Alternatively, the adsorption capacity of this system increased with the addition of ionizable comonomers such as acrylic acid, methacrylic acid, and amine derivatives. For example, Naseem *et al.*[112] synthesized the same system together with a new comonomer (AAc). The adsorption capacity of the newly synthesized systems reached 434.8, 555.6, 476.2, and 526.3 mg g^{-1} for Cr(III) Pb(II), Cd(II), and Cu(II) ions, respectively. He *et al.*[86] also reported the preparation of core–shell microgel systems, in which both the core and shell region were made with organic polymers and the synthesized systems used for the adsorption of uranium ions from aqueous medium.

However, the release of the adsorbed material from the crosslinked network of the microgels and requirement of ultrafast centrifugation for their recycling are the main issues of these systems. These issues can be addressed by designing systems in which the adsorption of pollutants is done in the core region and the shell region controls the adsorbed material through adsorption process, which has not been reported to date.

4.2.3. Inorganic core encapsulated with metal ion containing organic shell. Inorganic core encapsulated with metal ion containing organic shell systems are rarely reported in the literature. In these systems, the core is made with inorganic materials and the shell with organic and metal ions. The adsorption capacity of these systems is very low due to the occupation of some space by already present cations. The electrostatic repulsion between the loaded cations and cationic adsorbents is also another reason for their low adsorption capacity. In this case, the adsorption capacity of these systems can be enhanced by removing the loaded cations from their shell regions, resulting in porosity in the system. This porosity increases the adsorption capacity of the systems. Zhao *et al.*[113] reported the synthesis of a core–shell system, in which the core consisted of Fe_3O_4 and shell chitosan-poly(acrylamide) CSa-P(AAm) together with Ca^{2+} ions. The adsorption quantity of Cr^{3+}, Cd^{2+}, Pd^{2+}, and Cu^{2+} ions from water by the synthesized systems was 4.64, 8.20, 18.56, and 37.84 mg g^{-1}, respectively. This adsorption capacity could be increased by removing the already loaded Ca^{2+} ions by treating them with dilute HCl solution. After removing the Ca^{2+} ions from the shell region, the adsorption capacity of the system increased rapidly due to the creation of empty space.

Limited research is available on this type of system. These systems are new and more suitable for the maximum removal of pollutants. Their adsorption capacity can further be enhanced by using comonomers together with monomers. Thus, readers can work on these systems for the adsorption of pollutants.

4.2.4. Organic polymer microgel encapsulated inorganic shell. In organic polymer microgel encapsulated inorganic shell systems, the core is made with organic crosslinked polymer and shell with inorganic materials. These types of core–shell microgels are frequently reported but rarely used for adsorption purposes. The silica region is not suitable for adsorption due to its nonpolar nature. Therefore, these systems are not used for adsorption. In this case, to make these systems suitable for adsorption, some polarity is induced by adding some polar materials on the surface of silica during synthesis. The polar materials make the systems suitable for adsorption. The other disadvantage of these systems is the reduction in the stimulus-responsive behavior of the microgel core due to the silica shell.[114] Therefore, the stimulus-responsive behavior of the microgel core does not increase the adsorption capacity of these core–shell systems. The stimulus-responsive behavior of the microgel core depends on the thickness of the silica shell region. If the thickness of the silica shell region is very high, then the responsive behavior of the microgels highly decreases. Alternatively, if the thickness of silica is very low, then the responsiveness decreases slightly from normal behavior.[115] Yao *et al.*[82] synthesized this type of core–shell microgel system. The surface of the silica shell region of the synthesized core–shell system was decorated with poly(etheramine) P(EAm) and used for the adsorption of CO_2. The synthesized system showed excellent adsorption capacity due to the linear polymer structure of P(EAm) on the surface of silica. This linear polymer structure provided more space for the storage of CO_2.

Core–shell microgel systems without any modification of the surface of silica shell are not very suitable for adsorption but their adsorption capacity can be enhanced by modification of the surface of the silica shell region. But the adsorbed pollutant can detach during centrifugation process which is used for recycling of adsorbent. Very limited research work is available on adsorption of pollutants by such systems. More research can be done on adsorption of such systems in the near future.

4.2.5. Organic polymeric core encapsulated with linear organic polymer shell. In organic polymeric core encapsulated with linear organic polymer shell systems, their core is made up of a crosslinked organic polymer and shell with a linear organic polymer. These systems are very important with respect to adsorption. The adsorption capacity of these systems is very high due to their large empty space, stimuli-responsive behavior (swelling/deswelling behavior), and electrostatic interactions. The adsorption capacity of these systems also depends on the concentration of their linear polymer shell. If a greater content of linear polymer material is used during their synthesis, then more active sites are available for the adsorption of pollutants and the efficiency of core–shell microgels reach the maximum level. Alternatively, if the concentration of linear polymer is low,

© 2024 The Author(s). Published by the Royal Society of Chemistry

then a low amount of pollutant is adsorbed due to the less chance of available space. For example, Chuang *et al.*[116] reported the synthesis of this type of core–shell system with a varying ratio of NIPr core and *N*-4-amino-2-methylene-4-oxobutanoic acid (NAMOBu) shell materials. They used the synthesized core–shell microgels for the adsorption of Cu^{2+} ions, where 80% removal of Cu^{2+} ions was achieved when the core : shell ratio is 9 : 1 and 85% when this ratio was 7 : 3. When the concentration of linear materials increased, then more active sites are available for adsorption of Cu^{2+} ions. Therefore, more Cu^{2+} ions are adsorbed on these core–shell systems.

These core–shell microgel systems are also rarely reported for the adsorption of pollutants. More work on these types of core–shell microgel systems can be possible in the near future due to their high efficiency for the adsorption of pollutants. The usage of ultra-fast centrifugation and leaching of adsorbed pollutants during recycling are the only issues associated with these systems, which can be resolved by increasing the density of core–shell microgels in different ways and need to be studied in the near future.

4.3. Homogenous inorganic–organic microgel composite

In homogenous inorganic-organic composite systems, the inorganic material (SiO_2, Fe_2O_3 or Fe_3O_4) is uniformly distributed in the crosslinked network of organic polymers. The inorganic materials are from SiO_2, Fe_2O_3 or Fe_3O_4, which is used to synthesize these types of systems. The adsorption capacity of these systems is very low compared to simple and core–shell microgels due to the lower availability of space for the adsorbate. In these systems, some space is occupied with inorganic materials. Therefore, a very small amount of adsorbate is adsorbed in these classes. Mlih *et al.*[117] synthesized an Fe_2O_3-decorated poly(acrylic acid-maleic acid) P(AAc-MAc) microgel composite. The synthesized system was used for the adsorption of copper(II) ions and lead(II) ions from water. The adsorption capacity of the synthesized systems increased with an increase in the pH of the medium due to the conversion of –COOH groups into $–COO^-$ ions. Due to swelling and more electrostatic interactions between the metal ions and carboxylate ions, more metal ions enter the sieves of the crosslinked network. Under normal or acidic conditions, a very small amount of metal cations can enter the sieves. Therefore, the adsorption is very low under these conditions.

Due to their low adsorption capacity, very little research work has been reported on these systems. The adsorption capacity of these systems can be increased by introducing linear polymers on the surface of inorganic–organic microgel composites. The linear polymer chain also adsorbs metal cations together with the surface of the composite. Therefore, the adsorption capacity increases from simple composite materials. Yao *et al.*[82] reported similar trends in the adsorption pattern of composite and composite systems with linear polymer on their surface.

4.4. Fe_3O_4-crosslinked organic polymer microgels

In Fe_3O_4-crosslinked organic polymer microgel systems, the organic monomer with or without comonomer is crosslinked with Fe_3O_4 (inorganic material). This type of microgel is rarely reported in the literature. The control of their size is the main issue associated with these systems because large-sized systems are formed during their synthesis. Therefore, the surface area of these types of microgels is very small. Therefore, the adsorption capacity of these systems is very low compared to the previously discussed classes. Jiang *et al.*[118] reported the preparation of this type of system and used it for the adsorption of lead(II) ions. However, due to its low porosity and low surface area, the microgel adsorbed a small amount of lead(II) ions. The synthesized system was pH dependent due to the presence of –COOH groups in its structure. Therefore, the adsorption capacity of this system was increased by adjusting the pH of the medium. Also, its easy recycling property is the main advantage of this system, which was simply recycled by applying a magnetic field, and then used again for the adsorption process.

5. Stimulus-responsive behavior of microgels

Microgels show swelling and deswelling behavior under various conditions. These conditions are explained below.

5.1. Temperature effect

Microgel particles possess a structure resembling that of a sponge, where their interstitial spaces are occupied by water molecules. These polymeric particles exhibit sensitivity to variations in temperature, as discussed in the studies by Arif *et al.*[119] and Arif.[120,121]

The temperature sensitivity of microgels arises from the interplay between the hydrophilic/hydrophobic interactions within the microgel network and that with the surrounding medium. Generally, hydrophilic interactions dominate over hydrophobic interactions at low temperature, while hydrophobic interactions dominate hydrophilic interactions at high temperature. The temperature after the rapid change in the hydrodynamic diameter of microgels is called the volume phase transition temperature (VPTT), which is fixed for pure microgels (only single monomer-containing microgels). For example, the VPTT value of *N*-isopropylacrylamide-based microgels is 32 °C. However, this value can be increased by adding a hydrophilic group-containing comonomer during the synthesis of microgels. Due to the increase in the content of hydrophilic-containing comonomers, the interactions of microgels with water molecules also increase. Therefore, the value of VPTT increases with an increase in the content of commoners. For example, Zhang *et al.*[122] synthesized NIPr-based microgels and studied the effect of the temperature of the hydrodynamic diameter (D_h) of the synthesized microgels. They obtained a VPTT of 32 °C for the synthesized microgels. To increase this value, Yang *et al.*[37] synthesized a microgel system, in which 1-vinyl imidazole (VIDa) was used as the comonomer together with NIPr monomer. After the addition of this comonomer, the VPTT value of the microgels shifted from 32 °C to 37.5 °C, which is equal to the human body temperature. Secondly, the prepared microgel system is the best source for drug delivery in

© 2024 The Author(s). Published by the Royal Society of Chemistry

human beings due to its VPTT of 37.5 °C (almost equal to the human body temperature). The effect of the temperature on the swelling and deswelling behavior of microgels can be divided into two types, as presented below.

5.1.1. Negative temperature effect. In this temperature effect, the relationship between the hydrodynamic diameter of microgels and temperature is inverse. The hydrodynamic diameter of microgels decreases with an increase in the temperature, while it increases with a decrease in temperature. This type of temperature effect on the hydrodynamic diameter of microgels is called the negative temperature effect. Strong interactions are present between the structure of microgels and water molecules at low temperature. This interaction decreases with an increase in the temperature of the medium and the hydrophobic interaction increases gradually with temperature. Therefore, the water molecules are released from the network of microgels. Consequently, the hydrodynamic diameter of microgels decreases with an increase in temperature. For example, Picard *et al.*[38] synthesized NIPr-based microgels (with or without acrylic acid). They obtained the D_h value of 630 nm (without acrylic acid) and 1070 nm (with acrylic acid) at 25 °C. Alternatively, the D_h values decreased to 290 nm (without acrylic acid) and 340 nm at 50 °C and pH 6, respectively. The D_h of acrylic acid-containing microgels is higher than that without acrylic acid due to the more hydrophilic character in the former than the latter case. Kureha *et al.*[123] also synthesized P(NIPr-AAc) microgels and studied the effect of temperature on their swelling and deswelling behavior. The hydrodynamic diameter of the microgel was found to be 1230 nm at 20 °C and 775 nm at 50 °C and pH 5, respectively.

5.1.2. Positive temperature effect. In this effect, the value of the hydrodynamic diameter of hybrid microgels increases with an increase in temperature. Under this condition, the hydrophobic interactions increase with an increase in temperature. Therefore, the microgel particles start to coagulate to form large-sized microgels, resulting in an increase in the hydrodynamic diameter of the microgel. The increasing hydrodynamic diameter behavior of microgels with an increase in temperature is called the positive temperature effect. Initially, the hydrodynamic diameter of microgels decreases with an increase in temperature due to the increase in hydrophilic interactions. However, in some microgels, the hydrodynamic diameter starts to increase again due to coagulation. This coagulation occurs due to the intermolecular hydrogen bonding between the particles of microgels. The temperature at which the microgel particles start to coagulate to form large-sized microgels is called the upper critical solution temperature (UCST). For example, Pany *et al.*[32] synthesized P(NIPr-AAc) microgels and studied their temperature effect. The hydrodynamic diameter of the microgels decreased with an increase in temperature initially (during conversion from a to b) due to the increase in hydrophobic interactions, as shown in Fig. 5. The hydrodynamic diameter started to increase due to the coagulation of the microgels by hydrophobic interactions (during conversion from b to c) after 35 °C in acidic medium (pH = 3) and 37.5 °C in basic medium (pH = 7), respectively. Similar trends were reported in P(NIPr) microgels by Backes *et al.*[124]

5.2. pH effect

The swelling and deswelling behavior of microgels at different medium pH values is called the pH effect. Based on their acidic/basic nature, microgels can be divided into two types, as given below.

5.2.1. Acidic microgels. Acidic microgels are those with the capacity to donate the protons from their structure in basic

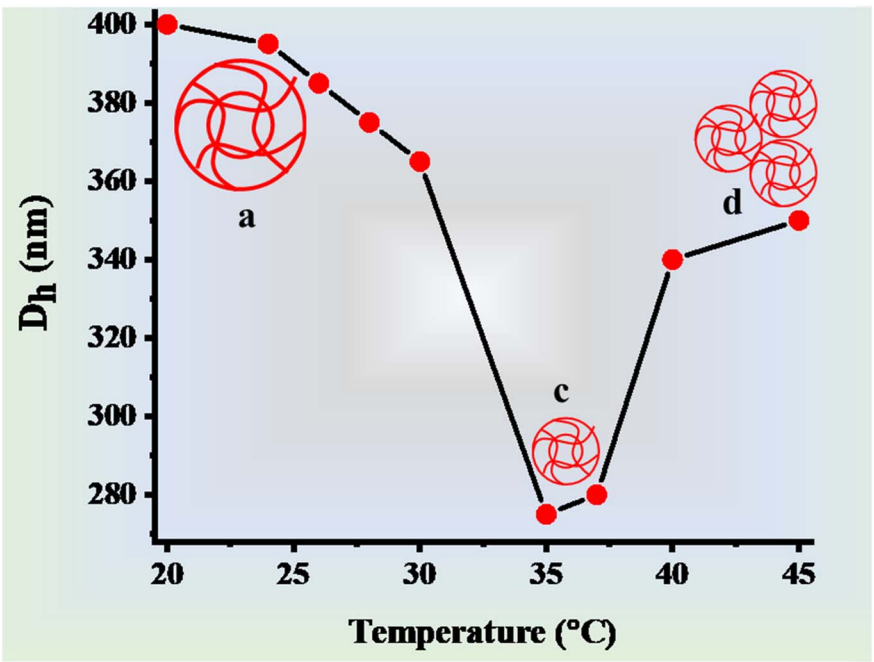

Fig. 5 Temperature effect on the swelling/deswelling behavior of P(NIPr-AAc) microgels.[32]

© 2024 The Author(s). Published by the Royal Society of Chemistry

medium. These microgels are acidic in nature because they have –COOH or –SO_3H groups in their structures. These acidic groups donate their protons under the condition of pH ≥ pK_a value of acidic moieties. Due to the donation of the protons from the structure of acidic microgels, their acidic groups are converted into anions. Electrostatic repulsion takes place due to the presence of the same charges in the structure of the microgels. Therefore, the size of the microgels increases due to this electrostatic repulsion, as shown in Fig. 6. Atta *et al.*[125] synthesized a poly(2-acrylamido-2-methyl propane sulfonic acid-*co*-acrylamide) P(AAMPSu-AAm) microgel with –SO_3H groups in its structure. Due to the presence of these groups in the structure of the synthesized microgel, it could easily donate the protons from the –SO_3H groups, resulting in the swelling state. The D_h value of the microgel was 895 nm at pH 4, 950 nm at 7, and 1193 nm at pH 9. This increasing trend in hydrodynamic diameter was due to the swelling behavior of the synthesized microgel (due to electrostatic repulsion). Rahman *et al.*[76] also reported the synthesis of poly(methacrylic acid) microgels with carboxylic groups present in their structures. Due to the presence of these carboxylic groups in their structures, the microgels could donate the protons from their structure, resulting in the formation of a swelling state. Similar behavior was observed by Sun *et al.*[126]

These types of microgels are the best adsorbents for cationic pollutants. Under basic condition, the microgels (adsorbents) are converted into anionic form, and in this form, they have the largest affinity towards cations. Therefore, the maximum number of cationic pollutants can be adsorbed under this condition. In contrast, these systems are the worst adsorbents for anionic pollutants under these conditions due to their electrostatic repulsion.

5.2.2. Basic microgels. Basic microgels have amino groups in their structures. These amino groups have the capacity to accept protons from the medium and convert their structures into cationic form. These types of microgels, which accept protons, are called basic microgels. Strong electrostatic repulsion takes place between the structures of the microgels, which results in the swelling state. Simply, these microgels are present in the swelling state in acidic medium and deswelling in basic medium, as shown in Fig. 6. Bao *et al.*[35] synthesized amino group-containing poly(dimethylamino)ethylmethacrylate P(DMAEMAc) microgels. The amino groups in these structures are basic in nature and have affinity for protons. Therefore, the microgels accept the protons in acidic medium to form cationic structures. In this form, electrostatic repulsion takes place and the hydrodynamic diameter of the microgels increases. Alfei *et al.*[127] also reported similar behavior of amino group-containing microgels.

This type of microgels has a positive charge in acidic medium and the most suitable adsorbent for anionic pollutants under this condition due to the strong electrostatic interaction between oppositely charged species. These microgels are in a swelling state under this condition, which is another advantage of this type of microgel. However, they are poor adsorbents for cationic pollutants under these conditions due to electrostatic repulsion.

5.3. Ionic strength

The presence of ionic concentrations also affects the swelling and deswelling behavior of microgels. The structure of microgels contains polar moieties, which produce partial charges in their structure. These polar moieties have affinities towards cations and anions. Due to this interaction, the polar parts can come close to each other by electrostatic attraction in oppositely charged parts or move away from each other by electrostatic repulsion in the same charged parts of microgels. Therefore, the hydrodynamic diameter of microgels can be affected by introducing ionic species. Alternatively, charged microgels are strongly affected by the addition of salts due to ion–ion interactions. The oppositely charged ions attracted each other due to ion–ion interactions and same-charged ions strongly repel each other. In this way, the hydrodynamic diameter of microgels is significantly affected by the addition of salts in the dispersion of microgels. The interactions between the ionic species are stronger than partial charge-containing species. Therefore, the structure of charged microgels is greatly affected by the addition of salt. Chen *et al.*[128] synthesized a core–shell microgel system consisting of poly(acrylic acid) P(AAc) and polyethersulfone P(ESFo). The mobility of the microgel decreased with an increase in the concentration of NaCl. Na^+ ions enter the structure of the microgel due to the ion–dipole interaction at a low pH value because the –COOH groups are present in protonated form. However, at a high pH value (pH ≥ pK_a of AAc), the –COOH groups of the microgels were present in the deprotonated form. Electrostatic repulsion occurred in these carboxylate ions. These carboxylates ions interact with the Na^+ ions. Due to this interaction, the carboxylate ions come close to

Fig. 6 Effect of pH on both acidic and basic microgels.

© 2024 The Author(s). Published by the Royal Society of Chemistry

each other and the hydrodynamic diameter of the microgel decreases. Consequently, the adsorption capacity of the microgel decreased with an increase in salt content due to the decrease in the mobility of the microgel. Truzzolillo *et al.*[129] also studied the effect of salt concentration on the swelling and deswelling behavior of P(NIPr)-based microgels. Similar trends in swelling behavior were observed.

The presence of ionic salts reduces the mobility and hydrodynamic diameter of microgels. Therefore, the presence of ionic salts reduces the adsorption capacity of microgels. It also reduces their thermo-responsive behavior due to their strong interactions with metal cations.

6. Adsorption capacity-enhancing factors of microgels

The inherent responsiveness of microgels makes them highly effective adsorbents for the removal of pollutants from the environment. A notable advantage of using microgels as adsorbents is their capacity for regeneration and use in multiple cycles.[27] Compared to macrogels, microgels are the preferred choice due to their smaller particle size, resulting in a larger surface area.[87] Because adsorption predominantly takes place on surfaces, this extensive surface area facilitates the effective capture of a significant quantity of contaminants during adsorption and desorption processes involving heavy metals and dyes when utilizing microgel adsorbents.

Previous studies have established that metal cations readily form complexes with functional group-containing nitrogen and oxygen in microgels.[130–132] The metal cations are electron-deficient species, and this deficiency of metal cations is fulfilled by getting electrons from electron-donating sites of microgels through coordinate covalent bonds. Similarly, other pollutants such as organic dyes and anions can also be removed by microgels. Polar parts are present in the structure of microgels. These polar parts can interact with organic dyes and separate them from water through hydrogen bonding or ion–dipole interactions. Anions can also be adsorbed on the surface of microgels through ion–dipole interactions. The amount of adsorbate on the surface of the adsorbent depends upon various factors, and the details of these factors are presented below.

6.1. Temperature

The temperature of the surrounding environment plays a pivotal role in modulating the adsorption capacity of microgels, primarily because of their thermo-responsive characteristics, as discussed in Section 5.1. The hydrodynamic diameter (D_h) of thermo-responsive microgels are significantly affected by a variation in temperature. Generally, the diameter of microgels decreases with an increase in temperature due to their increase in hydrophobicity. Therefore, the maximum adsorption of pollutants can be achieved in the swelling state, whereas the lowest at high temperature. Generally, high temperature is used for removing the loaded pollutants from the sieves of microgels. Pany *et al.*[32] reported the synthesis and use of thermo-responsive P(NIPr-AAc) microgels for the adsorption of MBl. 87% adsorption was observed at 20 °C and 63% at 50 °C due to the deswelling behavior as shown in Fig. 7. Similarly, Kureha *et al.*[123] also used P(NIPr-AAc) microgels for the adsorption of RG. 58 mg g^{-1} of RG was adsorbed by the synthesized microgels at 20 °C, while 41 mg g^{-1} at 40 °C due to the shifting of the microgels from the swelling state to deswelling state.

Naseem *et al.*[133] synthesized and used P(NIPMe-AAc) microgels as adsorbents for the adsorption of copper and cobalt ions from water and studied of the effect of temperature on their adsorption properties. The adsorption decreased with an increase in temperature from 15 °C to 50 °C. As the temperature increased, the kinetic energy of the adsorbate molecules also increased. Due to this increase in kinetic energy, the effect of the interactions decreased. Consequently, a smaller number of pollutants was absorbed on the surface of the adsorbate. This is

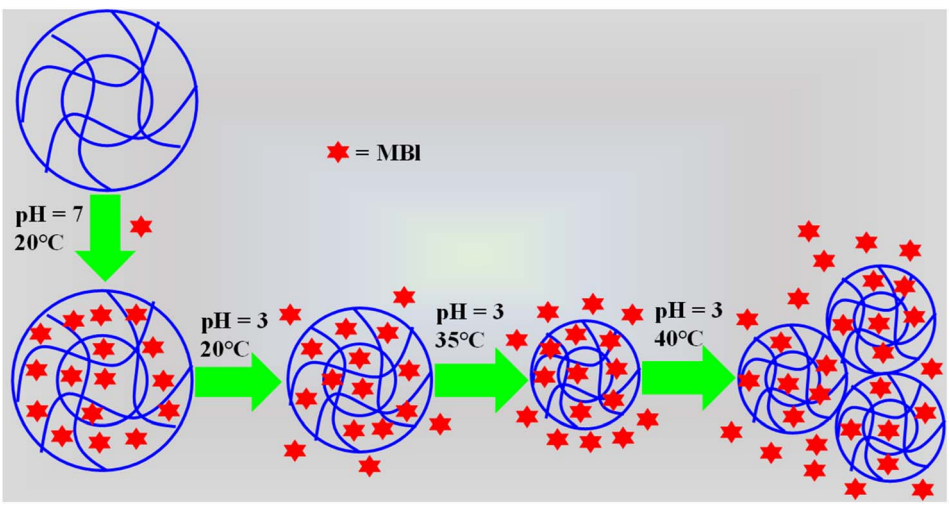

Fig. 7 Effect of temperature on methylene blue dye loading/releasing from P(NIPr-AAc) microgels in the temperature from 20 °C to 40 °C at pH 3.[32]

© 2024 The Author(s). Published by the Royal Society of Chemistry

also another reason for the lower adsorption of pollutants on the surface of microgels.

6.2. Mobility

Mobility is also an important factor affecting the adsorption of pollutants. Mobility refers to the process of pollutants entering and leaving the crosslinked polymeric network of microgels. Microgels adsorb pollutants on their surface first, and then these pollutants start to penetrate the crosslinked network, leaving empty space. This empty space is further occupied by other pollutant molecules. Consequently, the adsorption capacity of microgels is controlled by this penetration of pollutants from their surface. Therefore, the mobility of pollutants also affects their adsorption, which decreases with the microgels converting from the swelling state to deswelling state. In the swelling state, mobility occurs very easily due to the large empty space in the microgels. Conversely, this empty space decreases with the swelling state converting into the deswelling state. In the deswelling state, the mobility of pollutants decreases, and therefore the adsorption capacity of microgels also decreases. The conversion of the swelling state to the deswelling state or deswelling state to swelling state occurs by changing the environment of the medium such as pH, ionic strength, content of crosslinker, and temperature. Picard *et al.*[38] investigated the effect of temperature, content of crosslinker, ionic strength, and pH of the medium on the mobility of microgels, as shown in Table 1. The microgels are present in the swelling state at low temperatures, low content of crosslinkers, low ionic strength, and low pH (for basic microgels) or high pH (for acidic microgels), whereas in the deswelling state under the reverse conditions. Therefore, the adsorption capacity of microgels is high in the swelling state due to the high mobility.

6.3. Porosity of microgels

The adsorption capacity of any adsorbent is mainly dependent on the porosity of its surface. Similarly, the porosity of microgels also affects their adsorption capacity. High porosity means more pores are present on the surface of microgels, and therefore more empty space is available for adsorption. Porosity means the presence of holes in the surface of microgels, and the adsorbate can occupy these holes. If the porosity is high, then more adsorbate can enter these holes, while low amounts of adsorbate enter the holes if the porosity is low. Polar functional groups are also present in the structure for interaction with the adsorbate. The pollutants enter the holes due to this interaction and become trapped. Therefore, the adsorption capacity of microgel systems can be enhanced by producing porosity in their surface. For example, Ji[90] studied the adsorption capacity of non-porous and porous-based microgels. Anthocyanin was used as the adsorbate in this study. They placed the porous and non-porous microgels in solutions of anthocyanins separately and checked their adsorption capacities. The porous microgel adsorbed 31% of anthocyanin molecules, while that by the other adsorbent was 18% due to the greater empty space for the pollutants to occupy in the former. This porosity could be changed by changing the environment or by increasing the crosslinking. The porosity of the system increased with an increase in the crosslinking density. Therefore, the adsorption capacity of the microgel also increased with an increase in its crosslinking density. Cai *et al.*[91] synthesized crosslinked systems with various crosslinking densities. The porosity of the systems was checked by the BET technique. The porosity was low in the systems with a low crosslinking density and high in that with a high crosslinking density. The surface area of the pores increased from 637 $m^2\ g^{-1}$ to 1068 $m^2\ g^{-1}$ as the crosslinked density increased. They used the synthesized porous microgels for the adsorption of naphthalene and 1-naphthylaine. The highly crosslinked systems adsorbed more adsorbate due to their higher porosity than the other crosslinked materials. The porosity of the microgels could also be increased by converting their functional groups to other functional groups. Yun *et al.*[134] synthesized a nitrile group-containing microgel. The porosity of this system was determined to be 83%. After that, they converted the nitrile groups into carboxylic groups by treatment with NaOH. Due to this conversion, the porosity changed from 83% to 89%. The –COOH groups of the newly synthesized microgels were converted into $-COO^-$ ions. Due to carboxylate ions, electrostatic repulsion takes place and the porosity increased. Due to this increasing porosity and induction of negative charge in the structure of the microgels, their adsorption capacity significantly increased for anionic dyes, while rejecting cationic dyes due to electrostatic repulsion (due to same charges on microgels and pollutants).

6.4. Nature of medium

The solvent also affects the adsorption capacity of microgels. Microgels have a crosslinked network and the solvent can move in and out of these crosslinked networks. This movement of solvents into and out of these crosslinked networks affects the swelling and deswelling behavior of microgels. When the solvents enter the network, microgels are in the swelling state, whereas when the solvents leave the structure of microgels, they are converted into the deswelling state. Pollutants can also enter the crosslinked network of microgels together with these solvents. In the swelling state, more pollutants enter the microgels through adsorption. Therefore, the solvent directly affects the adsorption capacity of microgels. Due to this property of microgels, they microgels can be applied for the adsorption of

Table 1 Variation in mobility by the addition of comonomer[38]

Microgel	D_h (nm) pH = 3, T = 25 °C	D_h pH = 6, T = 50 °C	D_h pH = 6, T = 25 °C	Content of MBAc (mol%)	Electrophoretic mobility pH = 6 (10^{-4} $cm^2\ V^{-1}\ s^{-1}$)
P(NIPr)	630	290	630	2.5	-0.08 ± 0.03
P(NIPr-AAc)	660	340	1070	2.5	-1.49 ± 0.04

© 2024 The Author(s). Published by the Royal Society of Chemistry

water from humidity-containing areas. Guan *et al.*[135] synthesized hydroxypropyl cellulose-based microgels and used them as adsorbents for water. The adsorption of water increased with an increase in the contact time. The microgels showed 7.9–19.1 L kg^{-1} adsorption of water in one day by operating 24–36 cycles. The swelling behavior of microgels is different in different solvents. The microgels form a dispersion in water and a clear solution under alcoholic solvents. Therefore, the swelling behavior of microgels in alcoholic solvents is greater than in water medium. Boji *et al.*[88] synthesized VIDa-based microgels. The swelling and deswelling behaviors are greater in ethanol compared to water due to their greater solubility in ethanol than water, as shown in Fig. 8. Similarly, a mixture of solvents can also result in swelling and deswelling behavior under various conditions. Backes *et al.*[124] reported the synthesis of P(NIPr) microgels and studied their swelling and deswelling behavior in a mixture of solvents (water + ethanol). When the percentage of ethanol was greater than 30%, the hydrodynamic diameter of P(NIPr) first decreased with an increase in temperature up to 32 °C, and then again rapidly increased with an increase in temperature after 50 °C. As the temperature increased, the interaction of the microgels with water decreased, while it increased with ethanol. As reported in previous articles, the hydrophobic property of the microgels increased with an increase in the temperature. Ethanol solvent also has polar as well as non-polar parts in its structure. Therefore, the interaction between the microgel structure and ethanol increased with an increase in temperature due to van der Waals interactions. More prominent behavior was observed in alcohol together with water, following the order of methanol < ethanol < propanol due to the greater non-polar character. Similar behavior was also reported in another article by Backes.[136]

Kubiak *et al.*[89] applied a microgel system for the extraction of BPF, BPF, BPA, and BPB from a mixture of solvents (water + methanol). The percentage removal of these bisphenols increased with an increase in the percentage of methanol. These bisphenols have greater non-polar character and solubility in methanol. Therefore, these pollutants can easily enter the network of microgels together with methanol. Therefore, their percentage removal increased with an increase in the percentage of methanol. Among these pollutants, BPB has the most nonpolar character. Therefore, a greater amount of bisphenol is adsorbed than the other pollutants.

6.5. Phase of adsorbate and adsorbent

The phase of the adsorbent and adsorbate also affects the percentage removal of pollutants from the environment. Generally, the interaction between liquid phases is greater than gas phases. The kinetic energy of molecules is low in the liquid phase. Therefore, the adsorbent and adsorbate can easily come to close to each other in the liquid phase, where a lot of distance is present between them in the gas phase. Therefore, the adsorption of pollutants increases in the liquid phase compared to the gas phase. For example, Xie *et al.*[94] synthesized calix[4]pyrrole-based microgels and used them for the adsorption of iodine. The microgel adsorbed 3.38 g g^{-1} of iodine in the gas phase, while 7.814 g g^{-1} of iodine in aqueous medium. The

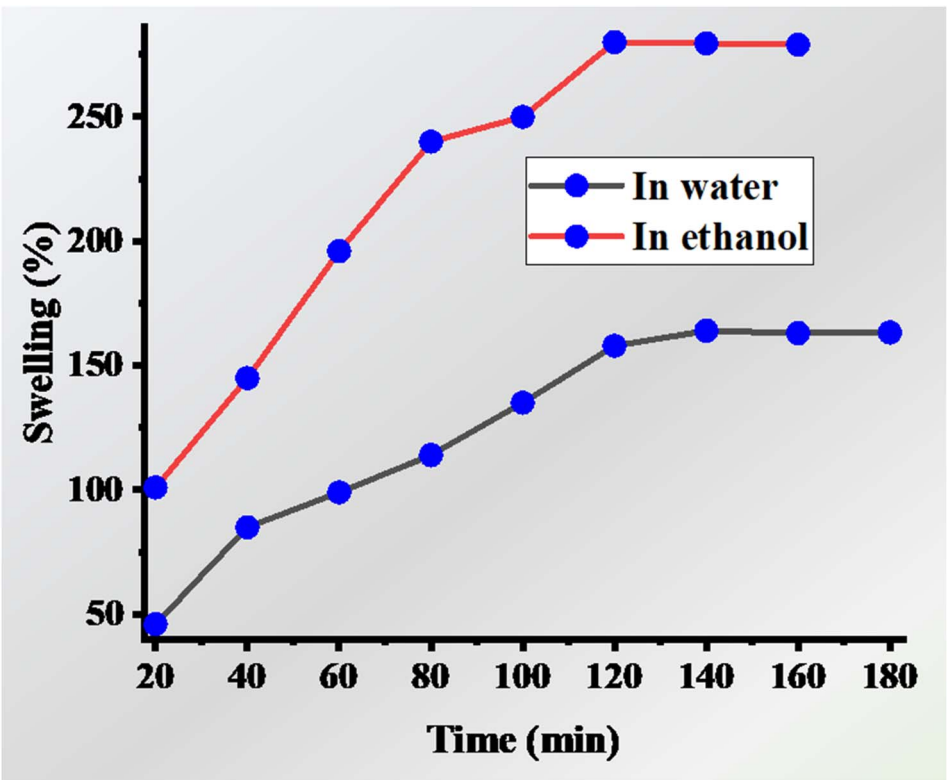

Fig. 8 Swelling behavior of VIDa-based microgels in ethanol (represented with red line) and water (represented with black line).[88]

© 2024 The Author(s). Published by the Royal Society of Chemistry

microgel removed 93.2% of iodine from water. Pollutants present in the gas phase such as CO_2,[82] H_2,[93] CH_4,[83] and SO_2 (ref. 137) can also be removed with the help of microgels. Frequently, the structure of microgels have nitrogen atoms and they can donate electron pairs from their nitrogen atoms. The hydrodynamic diameter of microgels increases with the adsorption of CO_2 and decreases after purging with N_2 gas. CO_2 reacts with water molecules to form H_2CO_3. This is an acid and donates a proton to the nitrogen atom of microgels. Nitrogen atoms have positive charges after accepting protons. Electrostatic repulsion takes place due to the same charges. Therefore, the hydrodynamic diameter of microgels increases. After purging with nitrogen, the CO_2 molecules come out from the crosslinked network of microgels, resulting in a decrease in their hydrodynamic diameter. CO_2-loaded microgels can also be used for the adsorption of other pollutants selectively. These microgels have a positive charge in their structure. Therefore, they adsorb anionic pollutants rather than cationic or non-ionic pollutants. Guo *et al.*[138] synthesized amino group-containing microgels. The hydrodynamic diameter of the synthesized microgels was 173 ± 37 μm in CO_2 and 48 ± 14 μm in N_2. The synthesized microgels showed high adsorption capacity in a CO_2 environment due to their swelling state and electrostatic interaction for anionic dyes. Yang *et al.*[139] and Avais *et al.*[83] also synthesized amino group-containing microgels and applied them for the adsorption of CO_2. The adsorption capacity of these microgels was found to be excellent.

6.6. Content of crosslinkers in microgels

The adsorption capacity of microgels is also controlled by the concentration of crosslinker used during their synthesis. When a large content of crosslinker is used, then a greater crosslinking density is present in the structure of microgels. Due to this greater crosslinking density, the mesh area (empty apace) in the crosslinked structure of microgels decreases. Therefore, less water molecules can enter the crosslinked network, and the difference in the hydrodynamic diameter of microgels in the swelling and deswelling state decreases. Meanwhile, the swelling and deswelling behavior of microgels decreases with an increase in the content of crosslinker. The hydrophobic nature of microgels increases with an increase in their crosslinking density. Therefore, the value of VPTT decreases with an increase in the content of crosslinker. Another disadvantage of a high content of crosslinker is the non-uniformity in sieves (mesh area). The crosslinking density is high in some areas compared to other areas in the structure of microgels. This effect also reduces the adsorption capacity of microgels. Kyrey *et al.*[107] investigated the effect of crosslinker content on the crosslinking density of microgels. The hydrophobic property is high in the region where the crosslinking density is high, whereas hydrophilic in the region where the crosslinking density is low. Therefore, more water molecules can enter the region where the crosslinking density is low, and more pollutants can also be adsorbed in this region. Therefore, a low content of crosslinker makes microgels more suitable for adsorption. Wang *et al.*[140] synthesized 18-crown-6-based microgel systems. The VPTT value of the synthesized microgels decreased with an increase in the content of crosslinker due to the increasing hydrophobic content (crosslinker). The adsorption of metal ions is higher by these microgels, which had a lower content of crosslinker. Joshi *et al.*[104] examined the effect of crosslinker content on the adsorption capacity of microgels. They used the synthesized microgels for the adsorption of uranyl ions from water. The microgels with 2.5% content of crosslinker swelled less than that with 0.65% of crosslinker content. Therefore, microgels with a lower crosslinker content have a greater mesh area for the adsorption of metal ions. Therefore, the adsorption capacity of microgels with a lower content of crosslinker is higher than that with a higher content of crosslinker.

6.7. pH of medium

The pH level of the solution plays a crucial role in adjusting the adsorption capacity of microgels for various pollutants. This factor significantly impacts both the behavior of the pollutants and the functionalities of the microgel network. The pH of the medium converts the structure of microgels into acidic or basic form by accepting or donating protons from their structures, respectively. Acidic microgels donate the protons from their structure to form anions. The anionic form of acidic microgels have strong affinity towards cationic pollutants due to the strong electrostatic interactions between the oppositely charged species but repel anionic pollutants due to their same charges. Similarly, basic microgels obtain positive charges in their structure by accepting protons. Cationic form microgels interact with the anionic pollutants due to the opposite charges on both the adsorbate and adsorbent species. Consequently, the pH of the medium affects the interactions presents between the adsorbate and absorbent together with the swelling and deswelling behavior, as discussed in Section 5.2.

The pH of the medium also affects the structure and electronic cloud of pollutants. Acidic dyes donate their protons in basic medium and basic dyes accept protons under acidic conditions. Therefore, the creation of a charge in the structure of pollutants results in a variation in the electrostatic interaction between the adsorbate and absorbent. In basic medium, metal cations start to form insoluble metal hydroxides, resulting in a reduction in metal cations in the medium. Therefore, the adsorption of cations decreases. Kubilay *et al.*[87] synthesized pol(ethyleneimine)-based microgels, cryogels and macrogels. They used these systems for the adsorption of chromate ions and arsenate ions. These systems adsorbed these anions due to the positive charges in their structure (under acidic condition). The adsorption capacity of the microgel systems was found to be greater than the cryogel and macrogel systems due to their smaller size and larger surface area. A greater amount of dichromate ions was adsorbed compared to arsenate ions because dichromate ions have more oxygen than arsenate. Therefore, more electrostatic interactions are present in dichromate ions and positively charged microgels. Allahyar *et al.*[141] synthesized carboxylic-group containing microgels. The synthesized microgels were applied to adsorb silver ions. The adsorption of silver ions increased with an increase in the pH value of

© 2024 The Author(s). Published by the Royal Society of Chemistry

the medium due to the conversion of the carboxylic groups into carboxylate ions. In this form, microgel had greater affinity towards silver ions. Therefore, the adsorption capacity of microgels increases with an increase in the pH of the medium. Zhang *et al.*[30] also reported the effect of pH on the adsorption of metal (Cu^{2+}, Fe^{3+}) ions on the surface of microgels. The microgels had acidic groups (–COOH, $–SO_3H$) in their structure. Therefore, the adsorption capacity of the microgels increased with an increase in the pH of the medium due to their conversion into deprotonated forms, as shown in Fig. 9. The adsorption capacity of the microgels was greater for Fe^{3+} ions than Cu^{2+} ions due to their higher charge density and smaller ionic radius. The adsorption capacity decreased after pH 5 due to the formation of insoluble metal hydroxides of metal ions (Fe^{3+} ions and Cu^{2+} ions).

6.8. Ionic strength

The ionic strength also affects the adsorption capacity of microgels. When salts such as NaCl are added to a dispersion of microgels, then the polar parts of the microgels interact with the Na^+ ions. Due to this interaction, the size of the microgels is also reduced. This decreasing behavior in the hydrodynamic diameter of microgels reduces their loading capacity by decreasing the mesh area. The insertion of Na^+ ions into the sieves of microgels produces resistance for the loading of other cationic pollutants due to electrostatic repulsion. The size of Na^+ ions is very small compared to heavy metal ions. Therefore, strong electrostatic interactions are present between these ions and the polar or anionic parts of microgels. Therefore, it is not possible to replace Na^+ ions with other heavy metal ions or cationic dyes. Therefore, the ionic strength reduces the adsorption capacity of microgels. The reduction in adsorption capacity of microgels depends on the content of NaCl. This reduction is greater if the content of NaCl is high and lower if the content of NaCl is small. Chen *et al.*[128] synthesized core–shell microgels and examined their adsorption capacity for different dyes (MBl, methyl violet (MVi), RB, Mor, and amaranth red (ARe)). The adsorption capacity of the core–shell microgels was higher for cationic dyes (MBl, MVi, RB) than anionic dyes (ARe, and MOr) due to the electrostatic interactions. –COOH groups are present in the structure of the core–shell microgels, which are converted into carboxylate ions. Thus, these ionic microgels interacted strongly with cationic dyes compared to anionic dyes and they adsorbed more cationic dyes than anionic dyes. Among the cationic dyes, MBl was adsorbed the most due to the less non-polar benzene rings in their structure. The adsorption capacity of the core–shell systems decreased when the content of NaCl increased from 0 mol L^{-1} to 1.00 mol L^{-1}. Similar behavior was observed by Zhao *et al.*[113] They used different contents of $NaNO_3$ during the adsorption of heavy metal ions. The adsorption capacity of the microgels decreased with an increase in the content of $NaNO_3$ from 0 mol L^{-1} to 0.1 mol L^{-1}. Zhang *et al.*[142] used microgels as adsorbates on a solid surface. The effect of the content of NaCl on this adsorption process also showed similar behavior.

6.9. Adsorption time (agitation time)

The duration of agitation also has an influence on the adsorption capacity of microgels (adsorbents) during the adsorption of

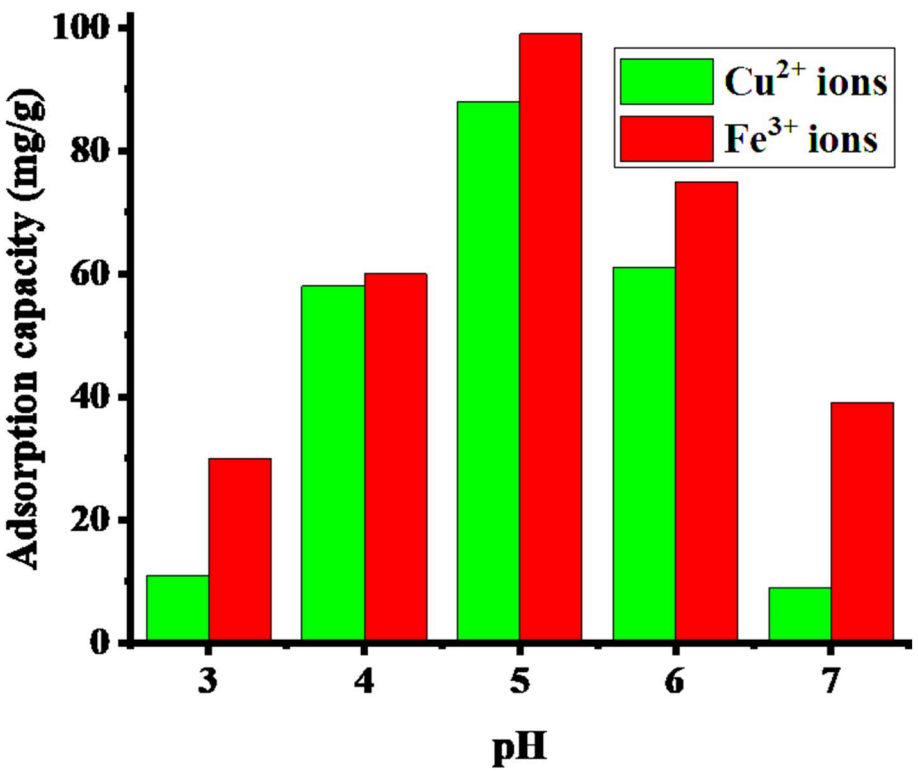

Fig. 9 Effect of pH on the adsorption capacity of P(AAm-CDo-AAMPSu) microgels.[30]

© 2024 The Author(s). Published by the Royal Society of Chemistry

various pollutants. At the beginning of the adsorption process, the adsorption of pollutants on the microgel increases rapidly because a greater number of functional groups on the microgels are available to interact with the pollutants. However, after a certain period, the removal of pollutants by the adsorbents (microgels) starts to increase at a slower rate. Under this condition, all the functional groups of the microgels (active sites) are occupied with pollutants and no functional groups are present for adsorption. The inner functional groups of microgels interact with the adsorbed pollutants on the surface. Therefore, the pollutants move to the inner side of the microgels due to this electrostatic interaction, leaving the functional groups for further adsorption. During this phase, the extraction of pollutants by the microgel follows the intraparticle diffusion mechanism. As time progresses further, the extraction of pollutants diminishes. This decline occurs because the functional groups of the microgels become saturated, and their capacity to adsorb additional pollutants diminishes. Alternatively, the rate of adsorption on the surface of microgels becomes equal to the rate of desorption from the surface of microgels. Yao *et al.*[143] applied microgels for the adsorption of MBl. The adsorption capacity of the microgels was high initially, gradually decreased, and then no adsorption occurred after a certain time. In the initial stage, a large number of active functional groups is present in the structure of microgels. Therefore, pollutants were adsorbed rapidly in the initial time from 0 min to 100 min. After 80 min, the adsorption rate slightly decreased. At this stage, MBl started to penetrate from the surface of the microgels into their sieves, leaving functional groups on their surface. These free groups further adsorb methylene groups. After 180 min, no further adsorption takes place. In this stage, the rate of adsorption and desorption becomes equal. One of us[101] also achieved similar behavior during the adsorption of cobalt(II) ions by homogenous microgels in one of my research projects. The percentage removal of Co^{2+} ions by the homogenous microgel with respect to time is presented in Table 2. Naseem *et al.*[81] also reported a similar effect of agitation time on the adsorption of dyes by a homogenous microgel system.

6.10. Content of adsorbate (pollutants)

The initial concentration of pollutants in the aqueous medium plays a significant role in the adsorption capacity of microgels. At lower pollutant concentrations, the adsorption capacity of the microgels was observed to increase proportionally with an increase in pollutant concentration. This relationship suggests that as more pollutants become available, more active sites on the microgels can be utilized for adsorption. However, it is noteworthy that this trend has its limits. Once the active sites on the microgels become saturated with pollutants, a further increase in pollutant concentration leads to a decline in the adsorption capacity of the microgels. In essence, the capacity of microgels to adsorb pollutants becomes restricted when all their available binding sites are already engaged. Yang *et al.*[37] investigated the effect of phosphate content on the adsorption capacity of microgels. They increased the content of phosphate ions from 0 mg mL^{-1} to 0.3 mg mL^{-1}, and observed that the adsorption capacity of the microgels increased with an increase in the content of phosphate ions. As the content of phosphate ions increased, more phosphate ions come into contact with the surface of the microgels. Therefore, the adsorption capacity of the microgels increased gradually. However, it did not increase further with an increase in the content of phosphate ions in the complete study. One of us[102] conducted a study investigating how the concentration of Cu^{2+} ions influenced the adsorption capacity of core–shell microgel systems, varying their concentrations from 10 to 80 mg L^{-1}. The adsorption increased with an increase in the content of copper(II) ions up to 40 mg L^{-1}, whereas no increasing trend was observed with a further increase in the content of copper from 40 to 80 mg L^{-1} due to all the active sites of the microgels being occupied with copper(II) ions. Zhang *et al.*[30] also observed similar results for the adsorption of Hg^{2+}, Fe^{3+}, and Cu^{2+} ions by microgels. Their research revealed that at lower metal ion concentrations, the adsorption capacity exhibited an increase in tandem with the rising metal ion concentration. However, as the concentration of metal ions further increased, a reduction in the adsorption capacity was observed.

6.11. Dose of microgels (adsorbents). The quantity of microgel administered during the adsorption process also plays a significant role in determining the percentage of pollutants removed from the aqueous medium. The number of active sites in microgels increases with an increase in their dose. Therefore, a large number of pollutants can be adsorbed on the surface of microgels. If the dose of microgel is low, then fewer active sites are available for the adsorption of pollutants. Therefore, a smaller number of pollutants is adsorbed on the surface of microgels. Bibi *et al.*[73] synthesized AAc-based microgels, and then employed the synthesized microgels for the adsorption of MBl. The adsorption capacity of the microgels increased with an increase in their dose from 12.5 in 100 mL to 100 mg in 100 mL. The adsorption capacity of these microgels decreased with an increase in microgel dose due to the increase in the number of –COOH groups, which are responsive for adsorption in the structure of microgels. These microgels showed excellent adsorption capacity due to the opposite charges between the structure of the microgels and methyl blue dye (cationic dye). Arif[36] also reported the synthesis of core–shell microgels and applied these core–shell systems for the adsorption of iron(III) ions. The percentage removal of iron(III) ions increased with an increase in the core–shell microgel dose. This increase provided more active sites for iron(III), ions resulting in an increase in the adsorption amount of iron(III).

Table 2 Percentage removal of Co^{2+} ions from water by homogenous microgels.[101]

Time of agitation	Percentage removal of Co^{2+} ions by microgels
15	94.413
30	94.901
45	94.982
60	95.912
75	96.021
90	96.210
105	96.218

© 2024 The Author(s). Published by the Royal Society of Chemistry

6.12. Nature of pollutant (adsorbate). When utilizing the same type of microgel adsorbent, it exhibits varying levels of effectiveness in the removal of various pollutants from aqueous solutions. Certain pollutants can be easily extracted from aqueous medium due to the formation of compatible interactions between them and the microgels. In contrast, some pollutants are not as readily removed because the necessary interactions for their extraction are absent. Chen *et al.*[27] synthesized amino and hydroxy group-containing microgels and applied them for the adsorption of heavy metal ions (Cd^{2+}, Zn^{2+}, Cu^{2+}, Pd^{2+}, Mn^{2+}, and Ni^{2+} ions). Among them, the synthesized microgels showed the highest removal for Pb^{2+} ions. The chelating ability of the microgels was higher for Pb^{2+} ions due to their electronegativity, charge density, mass to charge ratio, and size of the hydrated ion. One of our collaborators[81] synthesized and used the microgels for the adsorption of CRe, MBl, and RB dyes. Due to the presence of –COOH groups in the structure of the microgel systems, they removed a greater number of cationic dyes compared to anionic dyes due to electrostatic interactions at low temperature. The system adsorbed a greater number of molecules of CRe dye compared to MBl and RB at high temperatures. At low temperatures, the microgel is hydrophilic in nature, while this system is converted into hydrophobic at high temperatures. Therefore, the microgel adsorbs more at low temperatures and less at high temperatures. Chen *et al.*[128] also reported similar behavior for the adsorption of different dyes by core–shell microgels due to the interaction. The pH of the microgel dispersion also affects the adsorption capacity of microgels due to the variation in electrostatic interactions.

6.13. Addition of acidic or basic comonomers

The adsorption capacity of microgels can be increased with the addition of acidic or basic comonomers in their structure. These comonomers introduce positive or negative charges in the structure of microgels with a variation in the pH value of the medium. In this way, these comonomers produce more charge density in the structure, which is responsible for the greater electrostatic interaction between the pollutants and the charged microgels. Arif *et al.*[102] used a P(St)@P(NIPMe) microgel for the adsorption of copper ions. The rate of adsorption and adsorption capacity of the microgel were very low, which could be increased by adding acidic or basic comonomers in the shell region of the core–shell microgel. Therefore, one of our collaborators[112] synthesized P(St)@P(NIPMe-AAc) microgels. In this system, they introduced AAc in the microgel, and then used it for the adsorption of different metal ions together with copper(II) ions. The adsorption rate and adsorption capacity of this system were very high compared to the aforementioned system. Due to the introduction of AAc, more –COOH groups were present in the structure of the microgels. These groups have high electrostatic interaction towards copper(II) ions. Therefore, the adsorption rate of the microgels increased. Yang *et al.*[37] also reported a similar adsorption pattern using both P(NIPr) microgels and P(NIPr-VIDa) microgels for the adsorption of phosphate ions separately. The P(NIPr-VIDa) microgels showed better adsorption capacity and adsorption rate than the P(NIPr) microgels due to the polar and basic VIDa comonomers in the former.

6.14. Feed compositions of comonomers

The feed compositions of comonomers also affect the adsorption rate and adsorption capacity of microgels. Generally, the comonomers are responsive for increasing the rate of adsorption of pollutants. Their composition also affects the swelling and deswelling behavior of microgels together with their electrostatic interactions. Wang *et al.*[140] reported the synthesis of a microgel system together with 18-crown-6-based comonomers. The synthesized microgels were used for the adsorption of Pd^{2+} ions from water. The 18-crown-6 in the microgel was responsible for this adsorption. Due to the suitable radius of Pd^{2+} ions, they can be entrapped in this crown system. If the feed composition of this comonomer is increased, then more crowns are formed in the structure of the microgels. Therefore, more crowns are available for the adsorption of Pd^{2+} ions. In this way, the rate of adsorption increased with an increase in the feed of comonomers during the synthesis of the system. Yang *et al.*[37] reported the synthesis of microgels with different feed compositions of comonomer and used them for phosphate ion adsorption. Initially, the adsorption capacity increased due to the increase in basic component in the structure of the microgels. After a certain composition, the adsorption capacity of the microgels started to decrease. As the feed content of comonomer increased, the hydrodynamic diameter of the microgels increased. Therefore, more ions can enter the sieves of the microgels. If the content of this comonomer increases further, the swelling behavior of the microgels decreases. When the feed of the commoner increases further, more hydrophobic character is produced in the microgels. Therefore, the adsorption capacity of the microgels also decreases.

7. Adsorption isotherms

Various adsorption isotherms have been utilized to interpret the interaction between microgel adsorbents and pollutants. These isotherms not only help estimate the adsorption capacity of the adsorbents but also provide insights into the extent of adsorption. The commonly employed models include the Langmuir (LMu), Dubinin-Radushkevich (DRa), Freundlich (FLi), and Temkin (TKi) adsorption isotherms, which are frequently applied to investigate the adsorption process.

In the LMu model, adsorption involves the formation of a monolayer of adsorbate (pollutants) on the outer surface of the adsorbent (microgels), reaching an equilibrium state. Once this monolayer is formed, no further adsorption occurs on the outer surface. At this point, the rates of adsorption and desorption of the adsorbate from the outer layer of the adsorbent are equal.[144] DRa is a mathematical model used to describe the adsorption behavior of pollutants on a solid surface (microgels), particularly in the context of microporous materials.[132] The FLi model considers the multilayer adsorption of pollutants on a heterogeneous surface with varying adsorption affinities.[145] The TKi

© 2024 The Author(s). Published by the Royal Society of Chemistry

model deals with the interaction between the pollutant (adsorbate) and the surface of microgels (adsorbents).[144,146]

The mathematical form of the linear equations used for the LMu, FLi, DRa, and TKi adsorption isotherms are shown in eqn (1), (3), (4) and (7), respectively. In eqn (2), R_L is the separating factor, which is calculated using the Langmuir isotherm. R_L offers insights into the optimal adsorption of adsorbate on the surface of an adsorbent material. The R_L value falls in the adsorption range of 0–1. The value of ε is calculated with the help of eqn (5) and the mean free energy of adsorption, which is represented by E, is achieved with the help of eqn (6).

$$\frac{C_e}{q_e} = \frac{C_e}{q_m} + \frac{1}{bq_m} \quad (1)$$

$$R_L = \frac{1}{1 + bC_o} \quad (2)$$

$$\ln q_e = \ln K_F + \frac{1}{n} \ln C_e \quad (3)$$

$$\ln q_e = -\beta\varepsilon^2 + \ln q_m \quad (4)$$

$$\varepsilon = RT \ln\left(1 + \frac{1}{C_e}\right) \quad (5)$$

$$E = \frac{1}{\sqrt{2\beta}} \quad (6)$$

$$q_e = B \ln C_e + B \ln A \quad (7)$$

where C_e (mg L^{-1}) signifies the concentration of pollutants in the solution phase, while q_e (mg g^{-1}) represents the quantity of pollutants adsorbed on the microgels at equilibrium. The parameter q_m (mg g^{-1}) represents the monolayer adsorption capacity, R_L is the separation factor, which indicates the linkage between the adsorbent and adsorbate and its value is in the range of 0–1, C_o indicates the initial concentration of adsorbate, and b corresponds to the LMu adsorption constant (L mg^{-1}), which is associated with the energy of adsorption. K_F (L g^{-1}) represents the FLi isotherm constant, and n is the heterogeneity factor. The n value provides insight into the favorability of the adsorption process. β stands for the isotherm constant associated with the adsorption energy and R represents the universal gas constant (8.314 J K^{-1} mol^{-1}). The value of E serves as an indicator of the character of the adsorption process. When E is less than 8 kJ mol^{-1}, it signifies a physisorption nature. If E falls in the range of 8–16 kJ mol^{-1}, it suggests an ion exchange mechanism. Conversely, when E exceeds 16 kJ mol^{-1}, it indicates chemisorption. Regarding the Temkin adsorption isotherm model, it provides insights into the interaction between the adsorbent and the adsorbate, where A (L g^{-1}) and B (dimensionless) represent the Temkin constants. Specifically, the constant B is equal to RT/b, where b (J mol^{-1}) is another Temkin constant associated with the heat of adsorption.

Isikver *et al.*[80] reported the synthesis of microgels and used them for the adsorption of dyes. They applied the Langmuir adsorption isotherms for the adsorption of dyes by the microgels. The structure of the microgels have both cationic and anionic parts. Due to the presence of both cationic and anionic parts in their structure, the microgels could adsorb both cationic and anionic dyes from the environment. The adsorption of dyes on the surface of the microgels occurred due to hydrogen bonding and electrostatic interaction. Xu *et al.*[147] synthesized a composite system of graphene oxide-microgel and made this system suitable for the adsorption of cationic, anionic, and non-ionic dyes. In the structure of the microgel composite, both positive (due to protonation of amino groups from allyl amine moieties) and negative charges (due to deprotonation of carboxylic groups from graphene oxide moieties) are present. They also applied the LMu model to the adsorption process at various temperatures. Kureha *et al.*[123] also synthesized homogenous microgel systems and investigated their adsorption capacity for different dyes. They adsorbed EY, Rose Bengal (RBe), Erythrosine (ESi), Phloxine (PXi), OII, and Tartrazine (TTZi) dyes on the synthesized microgels. The FLi and LMu models were also applied to the adsorption of dyes. The microgels showed halogen bonding. Their methoxy groups for strong bonds with the halogen side of the dyes. Tatry *et al.*[148] and Qian *et al.*[33] also applied the Langmuir model for the adsorption by microgels. One of us[101] synthesized a homogenous microgel and investigated different adsorption isotherms such as LMu, Dra, FLi, and TKi on the adsorption of Co^{2+} ions by homogenous microgels.

8. Kinetics of adsorption process

The adsorption kinetics serves as a crucial physiochemical parameter for understanding the fundamentals of the adsorption process. Researchers make use of the pseudo-first-order (SFO), pseudo-second-order (SSO), and intraparticle diffusion (IPD) models to assess the rate of the adsorption process. The linear representation of the SFO, SSO, and IPD model kinetic models is expressed as follows:

$$\ln(q_e - q_t) = -k_1 t + \ln q_e \quad (8)$$

$$\frac{t}{q_t} = \frac{1}{k_2 {q_e}^2} + \frac{t}{q_e} \quad (9)$$

$$q_t = k_{int} t^{1/2} + 1 \quad (10)$$

where q_e (mg g^{-1}) and q_t (mg g^{-1}) denote the quantity of pollutants adsorbed on the microgel at equilibrium and at any given time, respectively. k_1 (1/s) and k_2 (g mg^{-1} s^{-1}) represent the rate constants for the SFO and the SSO kinetic models, respectively. K_{int} represents the intraparticle diffusion constant.

The intraparticle diffusion model is used to characterize the removal of pollutants from an aqueous solution when a porous microgel network is involved. This model breaks down the process into three key steps, as follows:

(a) The transportation of pollutants from the solution to the surface of the adsorbent.

(b) The diffusion of pollutants within the pores of the adsorbent.

© 2024 The Author(s). Published by the Royal Society of Chemistry

(c) The attachment of pollutants to the active sites within the microgel adsorbents.

In the initial phase, the surface of the adsorbent is unoccupied, and the adsorption kinetics can be viewed as a process primarily constrained by transport. This transport is governed by the diffusion of metal ions from the bulk solution to the surface of the adsorbent.

In the study by Arif *et al.*,[102] they observed that the adsorption of Cu^{2+} ions on the microgels adhered to the intraparticle diffusion model, as evidenced by the high R^2 (coefficient of determination) value of the intraparticle diffusion model. The intraparticle diffusion model serves to provide insights into the underlying mechanism of the adsorption process. Interestingly, their findings indicated that the adsorption of Cu^{2+} ions on the microgels occurred in three distinct steps. Initially, there was a rapid adsorption of Cu^{2+} ions due to the more active sites available for adsorption. In the second stage, the adsorbed ions penetrate the microgels and left empty surface for further adsorption. Subsequently, Cu^{2+} ions start to occupy the generated empty space.

Arif *et al.*[132] conducted a study on the kinetics of Cu^{2+} ion adsorption using core–shell microgels. Their observations revealed that the adsorption process was well described by SSO kinetics. When analyzing the intraparticle diffusion model, they found that it produced two distinct graphical segments. In the initial phase, a linear portion with the emergence of a plateau indicated the rapid adsorption of Cu^{2+} ions on the microgel surface. Subsequently, in the second phase, the less pronounced plateau depicted a slower adsorption process on the microgel adsorbent. This behavior suggested that the adsorption process was primarily driven by intraparticle diffusion, which served as the rate-determining step.

9. Thermodynamic aspect

The adsorption capacity of microgels can be influenced by the temperature of the medium.[149] Various thermodynamic parameters such as entropy change (ΔS°), enthalpy change (ΔH°), and free energy change (ΔG°) reveal the feasibility and nature of the adsorption process together with exothermic/endothermic nature. ΔS° and ΔH° can be determined by analyzing the intercept and slope of the plot ($1/T$ *vs.* $\ln K$) by employing eqn (11).

$$\ln K = -\frac{\Delta H^\circ}{RT} + \frac{\Delta S^\circ}{R} \tag{11}$$

The ΔG° value can be calculated by using eqn (12).

$$\Delta G^\circ = -RT \ln K \tag{12}$$

Eqn (11) and (12), R is the universal gas constant, K represents the equilibrium constant, and T denotes the temperature of the medium in Kelvin.

Naseem *et al.*[103] synthesized core–shell microgel systems and used them for the adsorption of Cu^{2+}, Cd^{2+}, and Cr^{3+} ions from water. The negative ΔG° values observed in metal ion adsorption indicate the spontaneous and feasible nature of the adsorption process. For all metal ions, an exothermic adsorption process is indicated by negative values of ΔH°, while a decrease in randomness at the interface of the adsorbate (metal ions) and adsorbent (core–shell microgels) is shown by negative values of ΔS°.

10. Conclusion and future directions

Different types of pollutants are present in the environment, which are very toxic to living organisms. These pollutants can be removed by adsorption processes and microgels are the best option as adsorbents due to their easy synthesis and stimulus-responsive behavior. Different types of adsorption isotherms can be applied to investigate the adsorption process. Kinetic studies are also important for the justification of the adsorption mechanism. The intra-particle diffusion model is best fitted to the adsorption of pollutants by microgels. Selectivity and high adsorption capacity of microgels can be achieved by the modification of the structures of microgels.

Microgels exhibit remarkable capacity for adsorbing various pollutants with high efficiency. The unique feature of microgels being sensitive to external stimuli allows for the adjustment of their adsorption capacity by altering factors such as temperature, ionic strength, and pH in the surrounding medium. Several factors, including dose of microgel, temperature, agitation duration, feed composition of monomers and comonomers during synthesis, pH level, choice of comonomers for functionalizing microgel adsorbents, acidic or basic comonomers, nature of both microgels and adsorbate, nature of medium, and the concentration of crosslinkers collectively govern the adsorption capacity of microgels for different types of pollutants. The substantial presence of functional groups within the microgel network significantly contributes to the enhanced adsorption of pollutants. Additionally, the adsorption of pollutants on microgel adsorbents can manifest as monolayer or multilayer adsorption, depending on both the characteristics of the microgel adsorbent itself and the nature of the specific pollutant.

Microgels and composite microgels demonstrate remarkable efficiency as adsorbents for eliminating pollutants from the environment; however, their relatively high production costs have limited their widespread application in large-scale water purification or pollutant removal efforts. Thus, there is a pressing need to develop methods for manufacturing microgels that can significantly reduce their cost. One approach is to explore copolymerization with various other monomers such as vinyl acetate, vinyl-imidazole, hydroxyl-ethylene methacrylate, vinyl-aniline and acrylic acid to fine-tune the properties of microgels, making them more cost-effective, while maintaining their effectiveness as adsorbents. It is worth noting that most of the reported microgels exhibit exceptional efficiency in removing small-sized metal ions compared to their larger counterparts. When AAc is copolymerized with various microgels, it tends to form a less compact structure. This structural characteristic can potentially contribute to cost reduction and improved performance when applied as adsorbents. The carboxylic acid functional groups of AAc are primarily situated on the surface of microgel particles rather than being embedded within the microgel network. Consequently, microgels polymerized with AAc have the potential to serve as more

© 2024 The Author(s). Published by the Royal Society of Chemistry

effective adsorbents for removing large-sized heavy metal ions and cationic organic dyes compared to microgels polymerized with MAAc. In the latter case, a denser, block-like structure is formed, with the functional groups predominantly located inside the microgel network. The adsorbed metal ions can be further studied by converting these ions into metal nanoparticles. The newly synthesized systems are more effective in catalytic reduction reactions. This is another advantage of this type of adsorption by microgels. Furthermore, there is an emerging need to investigate the copolymerization of microgels with various biomolecules to enable their biodegradation after they have been used for their intended lifespan. Additionally, exploring the interactions that occur between pollutants and the functional groups in microgels presents an avenue for enhancing the adsorption capacity of microgels.

List of abbreviations

NIPr	*N*-Isopropylacrylamide
AAc	Acrylic acid
NIPMe	*N*-Isopropylmethacrylamide
AAm	Acrylamide
P(NIPr)	Poly(*N*-isopropylacrylamide)
MAAc	Methacrylic acid
CRe	Congo red
MBl	Methylene blue
P(DAm)	Poly(diamine)
P(VAl)	Poly(vinyl alcohol)
VPTT	Volume phase transition temperature
P(DMAEMAc)	Poly(2-(dimethylamino)ethylmethacrylate)
P(ESFo)	Poly(ether sulfone)
MVi	Methyl violet
ARe	Amaranth red
NVCa	*N*-Vinylcaprolactam
AAMPSu	2-Acrylamido-2-methylpropane sulphonic acid
EY	Eosin Y
SDSu	Sodium dodecyl sulfate
RB	Rhodamine-B
MOr	Methyl orange
MBAc	*N*,*N*′-Methylene-bis-acrylamide
APSu	Ammonium per sulphate
OII	Orange II
SDSu	Sodium dodecyl sulphate
P(St)	Poly(styrene)
St	Styrene
CDo	Carbon dot
D_h	Hydrodynamic diameter
CSa	Chitosan
UCST	Upper critical solution temperature
P(EAm)	Poly(etheramine)
MAc	Maleic acid
BPA	Bisphenol A
BPB	Bisphenol B
BPF	Bisphenol F
BPE	Bisphenol E
VPy	4-Vinylpyridine

Conflicts of interest

There is no conflict of interest.

Acknowledgements

Muhammad Arif is thankful to University of Management and Technology, Lahore-54770, Pakistan.

References

1 Y. Vasseghian, S. Hosseinzadeh, A. Khataee and E.-N. Dragoi, The concentration of persistent organic pollutants in water resources: A global systematic review, meta-analysis and probabilistic risk assessment, *Science of The Total Environment*, 2021, **796**, 149000, DOI: 10.1016/j.scitotenv.2021.149000.

2 R. N. Bharagava, G. Saxena and S. I. Mulla, Introduction to Industrial Wastes Containing Organic and Inorganic Pollutants and Bioremediation Approaches for Environmental Management, in *Bioremediation of Industrial Waste for Environmental Safety*, Springer Singapore, Singapore, 2020, pp. 1–18. DOI: DOI: 10.1007/978-981-13-1891-7_1.

3 E. Lipczynska-Kochany, Humic substances, their microbial interactions and effects on biological transformations of organic pollutants in water and soil: A review, *Chemosphere*, 2018, **202**, 420–437, DOI: 10.1016/j.chemosphere.2018.03.104.

4 K. H. Vardhan, P. S. Kumar and R. C. Panda, A review on heavy metal pollution, toxicity and remedial measures: Current trends and future perspectives, *J. Mol. Liq.*, 2019, **290**, 111197, DOI: 10.1016/j.molliq.2019.111197.

5 J. Ma, Y. Yang, X. Jiang, Z. Xie, X. Li, C. Chen and H. Chen, Impacts of inorganic anions and natural organic matter on thermally activated persulfate oxidation of BTEX in water, *Chemosphere*, 2018, **190**, 296–306, DOI: 10.1016/j.chemosphere.2017.09.148.

6 M. Ismail, K. Akhtar, M. I. Khan, T. Kamal, M. A. Khan, A. M. Asiri, J. Seo and S. B. Khan, Pollution, Toxicity and Carcinogenicity of Organic Dyes and their Catalytic Bio-Remediation, *Curr. Pharm. Des.*, 2019, **25**, 3645–3663, DOI: 10.2174/1381612825666191021142026.

7 R. Jiang, M. Wang, W. Chen and X. Li, Ecological risk evaluation of combined pollution of herbicide siduron and heavy metals in soils, *Sci. Total Environ.*, 2018, **626**, 1047–1056, DOI: 10.1016/j.scitotenv.2018.01.135.

8 S. A. Kraemer, A. Ramachandran and G. G. Perron, Antibiotic Pollution in the Environment: From Microbial Ecology to Public Policy, *Microorganisms*, 2019, **7**, 180, DOI: 10.3390/microorganisms7060180.

9 Sakshi, S. K. Singh and A. K. Haritash, Polycyclic aromatic hydrocarbons: soil pollution and remediation, *Int. J. Environ. Sci. Technol.*, 2019, **16**, 6489–6512, DOI: 10.1007/S13762-019-02414-3.

10 M. Elazzouzi, K. Haboubi and M. S. Elyoubi, Electrocoagulation flocculation as a low-cost process for

© 2024 The Author(s). Published by the Royal Society of Chemistry

pollutants removal from urban wastewater, *Chem. Eng. Res. Des.*, 2017, **117**, 614–626, DOI: 10.1016/j.cherd.2016.11.011.
11 W. Zhang, L. Xia, K. M. Deen, E. Asselin, B. Ma and C. Wang, Enhanced removal of cadmium from wastewater by electro-assisted cementation process: A peculiar Cd reduction on Zn anode, *Chem. Eng. J.*, 2023, **452**, 139692, DOI: 10.1016/j.cej.2022.139692.
12 S. Lu, L. Liu, Q. Yang, H. Demissie, R. Jiao, G. An and D. Wang, Removal characteristics and mechanism of microplastics and tetracycline composite pollutants by coagulation process, *Sci. Total Environ.*, 2021, **786**, 147508, DOI: 10.1016/j.scitotenv.2021.147508.
13 X. Meng, W. Xu, Z. Li, J. Yang, J. Zhao, X. Zou, Y. Sun and Y. Dai, Coupling of Hierarchical Al2O3/TiO2 Nanofibers into 3D Photothermal Aerogels Toward Simultaneous Water Evaporation and Purification, *Adv. Fiber Mater.*, 2020, **2**, 93–104, DOI: 10.1007/S42765-020-00029-9/FIGURES/7.
14 A. A. Al-Raad and M. M. Hanafiah, Removal of inorganic pollutants using electrocoagulation technology: a review of emerging applications and mechanisms, *J. Environ. Manage.*, 2021, **300**, 113696, DOI: 10.1016/j.jenvman.2021.113696.
15 A. Bashir, L. A. Malik, S. Ahad, T. Manzoor, M. A. Bhat, G. N. Dar and A. H. Pandith, Removal of heavy metal ions from aqueous system by ion-exchange and biosorption methods, *Environ. Chem. Lett.*, 2019, **17**, 729–754, DOI: 10.1007/s10311-018-00828-y.
16 W. T. Vieira, M. B. de Farias, M. P. Spaolonzi, M. G. C. da Silva and M. G. A. Vieira, Removal of endocrine disruptors in waters by adsorption, membrane filtration and biodegradation. A review, *Environ. Chem. Lett.*, 2020, **18**, 1113–1143, DOI: 10.1007/s10311-020-01000-1.
17 Y. Dai, N. Zhang, C. Xing, Q. Cui and Q. Sun, The adsorption, regeneration and engineering applications of biochar for removal organic pollutants: a review, *Chemosphere*, 2019, **223**, 12–27, DOI: 10.1016/j.chemosphere.2019.01.161.
18 G. T. Tee, X. Y. Gok and W. F. Yong, Adsorption of pollutants in wastewater *via* biosorbents, nanoparticles and magnetic biosorbents: a review, *Environ. Res.*, 2022, **212**, 113248, DOI: 10.1016/j.envres.2022.113248.
19 C. Petit, Present and future of MOF research in the field of adsorption and molecular separation, *Curr. Opin. Chem. Eng.*, 2018, **20**, 132–142, DOI: 10.1016/J.COCHE.2018.04.004.
20 V. B. Cashin, D. S. Eldridge, A. Yu and D. Zhao, Surface functionalization and manipulation of mesoporous silica adsorbents for improved removal of pollutants: a review, *Environ. Sci.*, 2018, **4**, 110–128, DOI: 10.1039/C7EW00322F.
21 K. Naseem, M. Arif, A. Anwar, S. Haider and M. S. Akhtar, Investigating adsorptive potential of Raphanus caudatus leaves biomass for methyl orange dye: isotherm and kinetic study, *Z. Phys. Chem.*, 2023, **237**, 1183–1205, DOI: 10.1515/ZPCH-2023-0255/DOWNLOADASSET/SUPPL/J_ZPCH-2023-0255_SUPPL_001.DOCX.
22 M. Chen, K. R. Kumrić, C. Thacker, R. Prodanović, G. Bolognesi and G. T. Vladisavljević, Selective Adsorption of Ionic Species Using Macroporous Monodispersed Polyethylene Glycol Diacrylate/Acrylic Acid Microgels with Tunable Negative Charge, *Gels*, 2023, **9**, 849, DOI: 10.3390/GELS9110849.
23 K. Phonlakan, P. Meetam, R. Chonlaphak, P. Kongseng, S. Chantarak and S. Budsombat, Poly(acrylic acid- co -2-acrylamido-2-methyl-1-propanesulfonic acid)-grafted chitosan hydrogels for effective adsorption and photocatalytic degradation of dyes, *RSC Adv.*, 2023, **13**, 31002–31016, DOI: 10.1039/D3RA05596E.
24 H. Mondal and M. Karmakar, An MXene-Grafted Terpolymer Hydrogel for Adsorptive Immobilization of Toxic Pb(II) and Post-Adsorption Application of Metal Ion Hydrogel, *Gels*, 2023, **9**, 827.
25 M. Arif, A tutorial review on bimetallic nanoparticles loaded in smart organic polymer microgels/hydrogels, *J. Mol. Liq.*, 2023, **375**, 121346, DOI: 10.1016/j.molliq.2023.121346.
26 A. Abbasi, I. Ahmad and S. Ikram, Exploration of Adsorption Efficiency Mechanism and Swelling Behavior of Novel Green Itaconic Acid Modified Gellan Gum Hydrogel Nanocomposite for the Removal of Noxious Dyes, *J. Polym. Environ.*, 2023, 1–22, DOI: 10.1007/S10924-023-03058-8/TABLES/5.
27 Y. Chen, T. Wang, J. Liu, J. Huang, G. Zhou and S. Hu, Synthesis of microgel-reinforced double network hydrogel adsorbent and its adsorption on heavy metals, *J. Chem. Technol. Biotechnol.*, 2023, **98**, 1260–1268, DOI: 10.1002/JCTB.7343.
28 S. He, J. Li, X. Cao, F. Xie, H. Yang, C. Wang, C. Bittencourt and W. Li, Regenerated cellulose/chitosan composite aerogel with highly efficient adsorption for anionic dyes, *Int. J. Biol. Macromol.*, 2023, **244**, 125067, DOI: 10.1016/j.ijbiomac.2023.125067.
29 H. P. Mota, R. F. N. Quadrado and A. R. Fajardo, Recyclable multi-network hDesign of self-healable and ydrogels for efficient and selective removal of cationic dyes, *Eur. Polym. J.*, 2023, **200**, 112487, DOI: 10.1016/j.eurpolymj.2023.112487.
30 D. Zhang, H. Li, J. Li, Z. Xu, H. Liu, Y. Zhao, X. Feng and L. Chen, Hydrophilic P(Am-CD-AMPS) microgel for visual detection and removal metal ions in aqueous solution, *Appl. Surf. Sci.*, 2020, **512**, 145668, DOI: 10.1016/j.apsusc.2020.145668.
31 D. Hopa, A. E. Kazzaz and P. Fatehi, Fabrication of carboxyalkylated lignin derived microgels for adsorbing heavy metals, *Ind. Crops Prod.*, 2022, **187**, 115482, DOI: 10.1016/j.indcrop.2022.115482.
32 B. Pany, A. Ghosh Majundar, M. Mohanty, K. P. Fyis, T. Dey, G. Tripathy, S. Bhat, J. Yamanaka and P. S. Mohanty, Polymerized stimulus-responsive microgels for the removal of organic dye from water, *J. Mol. Liq.*, 2023, **375**, 121267, DOI: 10.1016/j.molliq.2023.121267.
33 J. Qian, L. Zhou, X. Yang, D. Hua and N. Wu, Prussian blue analogue functionalized magnetic microgels with ionized chitosan for the cleaning of cesium-contaminated clay, *J.*

© 2024 The Author(s). Published by the Royal Society of Chemistry

Hazard. Mater., 2020, **386**, 121965, DOI: 10.1016/j.jhazmat.2019.121965.

34 M. Wiese, T. Lohaus, J. Haussmann and M. Wessling, Charged microgels adsorbed on porous membranes – A study of their mobility and molecular retention, *J. Membr. Sci.*, 2019, **588**, 117190, DOI: 10.1016/j.memsci.2019.117190.

35 Y. Bao, N. Gupta, C. Yang Chuah, Y. Nan Liang, C. P. Hu and X. Hu, Highly selective recovery of perfluorooctanoic acid from semiconductor wastewater *via* adsorption on pH-stimulated poly (dimethyl amino) ethyl methacrylate microgels, *Sep. Purif. Technol.*, 2022, **287**, 120479, DOI: 10.1016/J.SEPPUR.2022.120479.

36 M. Arif, Extraction of iron (III) ions by core–shell microgel for *in situ* formation of iron nanoparticles to reduce harmful pollutants from water, *J. Environ. Chem. Eng.*, 2023, **11**, 109270, DOI: 10.1016/j.jece.2023.109270.

37 J. Yang, B. Huang, Z. Lv and Z. Cao, Preparation and self-assembly of ionic (PNIPAM- co-VIM) microgels and their adsorption property for phosphate ions, *RSC Adv.*, 2023, **13**, 3425–3437, DOI: 10.1039/D2RA06678E.

38 C. Picard, P. Garrigue, M. C. Tatry, V. Lapeyre, S. Ravaine, V. Schmitt and V. Ravaine, Organization of Microgels at the Air–Water Interface under Compression: Role of Electrostatics and Cross-Linking Density, *Langmuir*, 2017, **33**, 7968–7981, DOI: 10.1021/ACS.LANGMUIR.7B01538/SUPPL_FILE/LA7B01538_SI_001.PDF.

39 M. Arif, Catalytic degradation of azo dyes by bimetallic nanoparticles loaded in smart polymer microgels, *RSC. Adv.*, 2023, **13**(5), 3008–3019, DOI: 10.1039/D2RA07932A.

40 R. Kumar, E. Davis, N. Kalita, D. Choudhury and R. Shunmugam, 4-Vinylpyridine derived physically crosslinked hydrogel as efficient mercury indicator, *Polym. Eng. Sci.*, 2023, **63**(12), 4118–4126, DOI: 10.1002/pen.26512.

41 H. Seto, H. Matsumoto, M. Shibuya, T. Akiyoshi, Y. Hoshino and Y. Miura, Poly(*N*-isopropylacrylamide) gel-based macroporous monolith for continuous-flow recovery of palladium(II) ions, *J. Appl. Polym. Sci.*, 2017, **134**, 44385, DOI: 10.1002/APP.44385.

42 K. Naseem, Z. H. Farooqi, R. Begum, M. Z. Ur Rehman, M. Ghufran, W. Wu, J. Najeeb and A. Irfan, Synthesis and characterization of poly(N-isopropylmethacrylamide-acrylic acid) smart polymer microgels for adsorptive extraction of copper(II) and cobalt(II) from aqueous medium: kinetic and thermodynamic aspects, *Environ. Sci. Pollut. Res.*, 2020, **27**, 28169–28182, DOI: 10.1007/S11356-020-09145-W/TABLES/4.

43 L. Yu, L. Jiang, S. Wang, M. Sun, D. Li and G. Du, Pectin microgel particles as high adsorption rate material for methylene blue: Performance, equilibrium, kinetic, mechanism and regeneration studies, *Int. J. Biol. Macromol.*, 2018, **112**, 383–389, DOI: 10.1016/j.ijbiomac.2018.01.193.

44 K. Naseem, Z. H. Farooqi, R. Begum, M. Ghufran, M. Z. U. Rehman, J. Najeeb, A. Irfan and A. G. Al-Sehemi, Poly(*N*-isopropylmethacrylamide-acrylic acid) microgels as adsorbent for removal of toxic dyes from aqueous medium, *J. Mol. Liq.*, 2018, **268**, 229–238, DOI: 10.1016/j.molliq.2018.07.039.

45 Y. Xiao, K. Pandey, A. Nicolás-Boluda, D. Onidas, P. Nizard, F. Carn, T. Lucas, J. Gateau, A. Martin-Molina, M. Quesada-Pérez, M. Del Mar Ramos-Tejada, F. Gazeau, Y. Luo and C. Mangeney, Synergic Thermo- and pH-Sensitive Hybrid Microgels Loaded with Fluorescent Dyes and Ultrasmall Gold Nanoparticles for Photoacoustic Imaging and Photothermal Therapy, *ACS Appl. Mater. Interfaces*, 2022, **14**, 54439–54457, DOI: 10.1021/ACSAMI.2C12796/SUPPL_FILE/AM2C12796_SI_001.PDF.

46 M. Avais and S. Chattopadhyay, Hierarchical Porous Polymers *via* a Microgel Intermediate: Green Synthesis and Applications toward the Removal of Pollutants, *ACS Appl. Polym. Mater.*, 2021, **3**, 789–800, DOI: 10.1021/ACSAPM.0C01086/SUPPL_FILE/AP0C01086_SI_001.PDF.

47 D. Yu, Y. Wang, M. Wu, L. Zhang, L. Wang and H. Ni, Surface functionalization of cellulose with hyperbranched polyamide for efficient adsorption of organic dyes and heavy metals, *J. Cleaner Prod.*, 2019, **232**, 774–783, DOI: 10.1016/j.jclepro.2019.06.024.

48 S. Kumari, M. Avais and S. Chattopadhyay, Microgels as Smart Polymer Colloids for Sensing and Environmental Remediation, *ACS Appl. Polym. Mater.*, 2023, **5**, 1626–1645, DOI: 10.1021/ACSAPM.2C01947/SUPPL_FILE/AP2C01947_SI_001.PDF.

49 X. Zhou, X. Wu, H. He, H. Liang, X. Yang, J. Nie, W. Zhang, B. Du and X. Wang, Contrast-enhancing fluorescence detection of copper ions by functional fluorescent microgels, *Sens. Actuators, B*, 2020, **320**, 128328, DOI: 10.1016/j.snb.2020.128328.

50 Z. He, Q. Chen, Y. Luo, Y. He, Y. Zhang, T. Liu, W. Xu, J. Zhang, Y. Liu, L. Xiong, S. Wang and Z. Guo, Degradable CO_2-responsive microgels with wrinkled porous structure for enhanced, selective and recyclable removal of anionic dyes, Cr(VI) and As(V), *Eur. Polym. J.*, 2021, **149**, 110374, DOI: 10.1016/j.eurpolymj.2021.110374.

51 S. R. Safi, T. Gotoh, T. Iizawa and S. Nakai, Development and regeneration of composite of cationic gel and iron hydroxide for adsorbing arsenic from ground water, *Chemosphere*, 2019, **217**, 808–815, DOI: 10.1016/j.chemosphere.2018.11.050.

52 Z. Guo, Q. Chen, H. Gu, Z. He, W. Xu, J. Zhang, Y. Liu, L. Xiong, L. Zheng and Y. Feng, Giant Microgels with CO 2-Induced On-Off, Selective, and Recyclable Adsorption for Anionic Dyes, *ACS Appl. Mater. Interfaces*, 2018, **10**, 38073–38083, DOI: 10.1021/ACSAMI.8B13448/SUPPL_FILE/AM8B13448_SI_002.AVI.

53 T. Kureha and D. Suzuki, Nanocomposite Microgels for the Selective Separation of Halogen Compounds from Aqueous Solution, *Langmuir*, 2018, **34**, 837–846, DOI: 10.1021/ACS.LANGMUIR.7B01485/SUPPL_FILE/LA7B01485_SI_001.PDF.

54 Y. Wu, Y. Zhang, K. Wang, Z. Luo, Z. Xue, H. Gao, Z. Cao, J. Cheng, C. Liu and L. Zhang, Construction of Self-Assembled Polyelectrolyte/Cationic Microgel Multilayers and Their Interaction with Anionic Dyes Using Quartz

© 2024 The Author(s). Published by the Royal Society of Chemistry

Crystal Microbalance and Atomic Force Microscopy, *ACS Omega*, 2021, **6**, 5764–5774, DOI: 10.1021/ACSOMEGA.0C06181/ASSET/IMAGES/MEDIUM/AO0C06181_M001.GIF.

55 D. Yiamsawas, W. Kangwansupamonkon and S. Kiatkamjornwong, Lignin-Based Microgels by Inverse Suspension Polymerization: Syntheses and Dye Removal, *Macromol. Chem. Phys.*, 2021, **222**, 2100285, DOI: 10.1002/MACP.202100285.

56 Y. Y. Chuang, J. R. Deka, W. Y. Hsieh, S. P. Rwei, J. W. Shiu and T. F. Way, Synthesis and characterization of PNM@IAM core–shell microgels through inverse emulsion polymerization and its application for heavy metal ions capture, *J. Macromol. Sci., Part A: Pure Appl.Chem.*, 2023, **60**, 427–441, DOI: 10.1080/10601325.2023.2213699.

57 A. Kubiak, M. Mackiewicz, M. Biesaga and M. Karbarz, Highly efficient removal of bisphenols from aqueous solution using environmental-sensitive microgel, *J. Environ. Chem. Eng.*, 2021, **9**, 104947, DOI: 10.1016/J.JECE.2020.104947.

58 K. Naseem, Z. Hussain Farooqi, M. Zia Ur Rehman, M. Atiq Ur Rehman and M. Ghufran, Microgels as efficient adsorbents for the removal of pollutants from aqueous medium, *Rev. Chem. Eng.*, 2019, **35**, 285–309, DOI: 10.1515/REVCE-2017-0042/MACHINEREADABLECITATION/RIS.

59 C. R. China, M. M. Maguta, S. S. Nyandoro, A. Hilonga, S. V. Kanth and K. N. Njau, Alternative tanning technologies and their suitability in curbing environmental pollution from the leather industry: a comprehensive review, *Chemosphere*, 2020, **254**, 126804, DOI: 10.1016/j.chemosphere.2020.126804.

60 H. Deng, R. Wei, W. Luo, L. Hu, B. Li, Y. Di and H. Shi, Microplastic pollution in water and sediment in a textile industrial area, *Environ. Pollut.*, 2020, **258**, 113658, DOI: 10.1016/j.envpol.2019.113658.

61 E. M. Melchor-Martínez, R. Macias-Garbett, A. Malacara-Becerra, H. M. N. Iqbal, J. E. Sosa-Hernández and R. Parra-Saldívar, Environmental impact of emerging contaminants from battery waste: a mini review, *Case Stud. Chem. Environ. Eng.*, 2021, **3**, 100104, DOI: 10.1016/j.cscee.2021.100104.

62 K. Y. Kirichenko, I. A. Vakhniuk, V. V. Ivanov, I. A. Tarasenko, D. Y. Kosyanov, S. A. Medvedev, V. P. Soparev, V. A. Drozd, A. S. Kholodov and K. S. Golokhvast, Complex study of air pollution in electroplating workshop, *Sci. Rep.*, 2020, **10**, 1–14, DOI: 10.1038/s41598-020-67771-3.

63 M. T. Sikder, M. M. Rahman, M. Jakariya, T. Hosokawa, M. Kurasaki and T. Saito, Remediation of water pollution with native cyclodextrins and modified cyclodextrins: A comparative overview and perspectives, *Chem. Eng. J.*, 2019, **355**, 920–941, DOI: 10.1016/j.cej.2018.08.218.

64 B. Lellis, C. Z. Fávaro-Polonio, J. A. Pamphile and J. C. Polonio, Effects of textile dyes on health and the environment and bioremediation potential of living organisms, *Biotechnology Research and Innovation*, 2019, **3**, 275–290, DOI: 10.1016/J.BIORI.2019.09.001.

65 Z. Fu and S. Xi, The effects of heavy metals on human metabolism, *Toxicol. Mech. Methods*, 2020, **30**, 167–176, DOI: 10.1080/15376516.2019.1701594.

66 S. Muzaffar, J. Khan, R. Srivastava, M. S. Gorbatyuk and M. Athar, Mechanistic understanding of the toxic effects of arsenic and warfare arsenicals on human health and environment, *Cell Biol. Toxicol.*, 2022, **39**, 85–110, DOI: 10.1007/S10565-022-09710-8.

67 A. Ahmad and P. Bhattacharya, Arsenic in Drinking Water: Is 10 μg L^{-1} a Safe Limit?, *Curr. Pollut. Rep.*, 2019, **5**, 1–3, DOI: 10.1007/S40726-019-0102-7/METRICS.

68 A. A. Taylor, J. S. Tsuji, M. R. Garry, M. E. McArdle, W. L. Goodfellow, W. J. Adams and C. A. Menzie, Critical Review of Exposure and Effects: Implications for Setting Regulatory Health Criteria for Ingested Copper, *Environ. Manage.*, 2020, **65**, 131–159, DOI: 10.1007/S00267-019-01234-Y/TABLES/5.

69 A. Kumar, A. Kumar, M. Cabral-Pinto, A. K. Chaturvedi, A. A. Shabnam, G. Subrahmanyam, R. Mondal, D. K. Gupta, S. K. Malyan, S. S. Kumar, S. A. Khan and K. K. Yadav, Lead Toxicity: Health Hazards, Influence on Food Chain, and Sustainable Remediation Approaches, *Int. J. Environ. Res. Public Health*, 2020, **17**, 2179, DOI: 10.3390/IJERPH17072179.

70 S. Benkhaya, S. M' rabet and A. El Harfi, A review on classifications, recent synthesis and applications of textile dyes, *Inorg. Chem. Commun.*, 2020, **115**, 107891, DOI: 10.1016/j.inoche.2020.107891.

71 A. Gičević, L. Hindija and A. Karačić, Toxicity of azo dyes in pharmaceutical industry, *IFMBE Proc*, 2020, **73**, 581–587, DOI: 10.1007/978-3-030-17971-7_88/COVER.

72 J. Wu, Z. Feng, C. Dong, P. Zhu, J. Qiu and L. Zhu, Synthesis of Sodium Carboxymethyl Cellulose/Poly(acrylic acid) Microgels *via* Visible-Light-Triggered Polymerization as a Self-Sedimentary Cationic Basic Dye Adsorbent, *Langmuir*, 2022, **38**, 3711–3719, DOI: 10.1021/ACS.LANGMUIR.1C03196/SUPPL_FILE/LA1C03196_SI_001.PDF.

73 F. Bibi, M. Ajmal, F. Naseer, Z. H. Farooqi and M. Siddiq, Preparation of magnetic microgels for catalytic reduction of 4-nitrophenol and removal of methylene blue from aqueous medium, *Int. J. Environ. Sci. Technol.*, 2017, **15**, 863–874, DOI: 10.1007/S13762-017-1446-4.

74 S. Rahman, M. Ajmal and M. Siddiq, Micron sized anionic poly (methacrylic acid) microgel particles for the adsorptive elimination of cationic water pollutants, *Z. Phys. Chem.*, 2023, **237**, 121–145, DOI: 10.1515/ZPCH-2022-0147/MACHINEREADABLECITATION/RIS.

75 K. Murakami, A. Imai and A. Nakamura, Temperature dependence of aggregation behavior and dye adsorption of poly(*N*-isopropylacrylamide) hydrogel/mesoporous silica composites, *Colloids Surf. A Physicochem. Eng. Asp.*, 2023, **674**, 131944, DOI: 10.1016/j.colsurfa.2023.131944.

76 S. Rahman, M. Ajmal and M. Siddiq, Micron sized anionic poly (methacrylic acid) microgel particles for the adsorptive

© 2024 The Author(s). Published by the Royal Society of Chemistry

elimination of cationic water pollutants, *Z. Phys. Chem.*, 2023, **237**, 121–145, DOI: 10.1515/ZPCH-2022-0147/MACHINEREADABLECITATION/RIS.

77 K. Murakami, A. Imai and A. Nakamura, Temperature dependence of aggregation behavior and dye adsorption of poly(*N*-isopropylacrylamide) hydrogel/mesoporous silica composites, *Colloids Surf. A Physicochem. Eng. Asp.*, 2023, **674**, 131944, DOI: 10.1016/j.colsurfa.2023.131944.

78 M. Arif, Core-shell systems of crosslinked organic polymers: a critical review, *Eur. Polym. J.*, 2024, **206**, 112803, DOI: 10.1016/j.eurpolymj.2024.112803.

79 J. Xu, H. Qiao, K. Yu, M. Chen, C. Liu, W. Richtering and H. Zhang, Cu2+ tunable temperature-responsive Pickering foams stabilized by poly (*N*-isopropylacrylamide-co-vinyl imidazole) microgel: Significance for Cu2+ recovery *via* flotation, *Chem. Eng. J.*, 2022, **442**, 136274, DOI: 10.1016/j.cej.2022.136274.

80 Y. Işıkver, D. Saraydın and N. Karakuş, An Experimental and Computational Evaluation of the Interaction Between Intelligent Ampholyte Acrylamide/Acrylic Acid/2-(Acryloyloxy)ethyl Trimethylammonium Chloride Hydrogel and Dyes, *J. Polym. Environ.*, 2023, 1–19, DOI: 10.1007/S10924-023-03067-7/FIGURES/19.

81 K. Naseem, Z. H. Farooqi, R. Begum, M. Ghufran, M. Z. U. Rehman, J. Najeeb, A. Irfan and A. G. Al-Sehemi, Poly(N-isopropylmethacrylamide-acrylic acid) microgels as adsorbent for removal of toxic dyes from aqueous medium, *J. Mol. Liq.*, 2018, **268**, 229–238, DOI: 10.1016/j.molliq.2018.07.039.

82 D. Yao, T. Li, Y. Zheng and Z. Zhang, Fabrication of a functional microgel-based hybrid nanofluid and its application in CO_2 gas adsorption, *React. Funct. Polym.*, 2019, **136**, 131–137, DOI: 10.1016/j.reactfunctpolym.2018.12.025.

83 M. Avais and S. Chattopadhyay, Hierarchical Porous Polymers *via* a Microgel Intermediate: Green Synthesis and Applications toward the Removal of Pollutants, *ACS Appl. Polym. Mater.*, 2021, **3**, 789–800, DOI: 10.1021/ACSAPM.0C01086/SUPPL_FILE/AP0C01086_SI_001.PDF.

84 S. M. M. Ghani, N. E. Rabat, A. R. Abdul Rahim, K. Johari, A. A. Siyal and R. Kumeresen, Amine Infused Fly Ash Grafted Acrylic Acid/Acrylamide Hydrogel for Carbon Dioxide (CO2) Adsorption and Its Kinetic Analysis, *Gels*, 2023, **9**, 229, DOI: 10.3390/GELS9030229.

85 H. Qiu, J. Li, M. Wang, H. Zhang, J. Shen, J. Xie, Y. Wang and W. Wu, Insect-Inspired Strategy for Conferring Reversible, High Responsivity on Microgels to Dilute-Source CO2, *ACS Macro Lett.*, 2023, **12**, 767–772, DOI: 10.1021/ACSMACROLETT.3C00228/SUPPL_FILE/MZ3C00228_SI_001.PDF.

86 P. He, M. Shen, W. Xie, Y. Ma and J. Pan, The Efficient and Convenient Extracting Uranium from Water by a Uranyl-Ion Affine Microgel Container, *Nanomaterials*, 2022, **12**, 2259, DOI: 10.3390/NANO12132259.

87 S. Kubilay, S. Demirci, M. Can, N. Aktas and N. Sahiner, Dichromate and arsenate anion removal by PEI microgel, cryogel, and bulkgel, *J. Environ. Chem. Eng.*, 2021, **9**, 104799, DOI: 10.1016/J.JECE.2020.104799.

88 M. Abbasi Boji and M. Ghorbanloo, Synthesis, characterization, and fabrication of silver nanoparticles in 1-vinyl imidazole-based hydrogels and their use in olefin oxidation, hydrogen generation, and oxo-anion adsorption, *Polym. Bull.*, 2022, **79**, 1257–1286, DOI: 10.1007/S00289-021-03937-X/FIGURES/12.

89 A. Kubiak, M. Maćkiewicz, M. Karbarz and M. Biesaga, Application of Microgel as a Sorbent for Bisphenol Analysis in Liquid Food Samples, *Appl. Sci.*, 2022, **12**, 441, DOI: 10.3390/APP12010441.

90 Y. Ji, Synthesis of porous starch microgels for the encapsulation, delivery and stabilization of anthocyanins, *J. Food Eng.*, 2021, **302**, 110552, DOI: 10.1016/j.jfoodeng.2021.110552.

91 Y. Cai, X. Wen, Y. Wang, H. Song, Z. Li, Y. Cui and C. Li, Preparation of hyper-crosslinked polymers with hierarchical porous structure from hyperbranched polymers for adsorption of naphthalene and 1-naphthylamine, *Sep. Purif. Technol.*, 2021, **266**, 118542, DOI: 10.1016/J.SEPPUR.2021.118542.

92 A. Sharma, S. H. Jung, N. Lomadze, A. Pich, S. Santer and M. Bekir, Adsorption Kinetics of a Photosensitive Surfactant Inside Microgels, *Macromolecules*, 2021, **54**, 10682–10690, DOI: 10.1021/ACS.MACROMOL.1C01994/SUPPL_FILE/MA1C01994_SI_003.MOV.

93 P. Ramirez-Vidal, F. Suárez-García, R. L. S. Canevesi, A. Castro-Muñiz, P. Gadonneix, J. I. Paredes, A. Celzard and V. Fierro, Irreversible deformation of hyper-crosslinked polymers after hydrogen adsorption, *J. Colloid Interface Sci.*, 2022, **605**, 513–527, DOI: 10.1016/j.jcis.2021.07.104.

94 L. Xie, Z. Zheng, Q. Lin, H. Zhou, X. Ji, J. L. Sessler and H. Wang, Calix[4]pyrrole-based Crosslinked Polymer Networks for Highly Effective Iodine Adsorption from Water, *Angew. Chem., Int. Ed.*, 2022, **61**, e202113724, DOI: 10.1002/ANIE.202113724.

95 M. Lopes, A. Sanches-Silva, M. Castilho, C. Cavaleiro and F. Ramos, Halophytes as source of bioactive phenolic compounds and their potential applications, *Crit. Rev. Food Sci. Nutr.*, 2023, **63**, 1078–1101, DOI: 10.1080/10408398.2021.1959295.

96 L. Zhang, J. Chu, B. Xia, Z. Xiong, S. Zhang and W. Tang, Health Effects of Particulate Uranium Exposure, *Toxics*, 2022, **10**, 575, DOI: 10.3390/TOXICS10100575.

97 M. Peacock, Phosphate Metabolism in Health and Disease, *Calcif. Tissue Int.*, 2020, **108**, 3–15, DOI: 10.1007/S00223-020-00686-3.

98 K. Szafulera, R. A. Wach, A. K. Olejnik, J. M. Rosiak and P. Ulański, Radiation synthesis of biocompatible hydrogels of dextran methacrylate, *Radiat. Phys. Chem.*, 2018, **142**, 115–120, DOI: 10.1016/j.radphyschem.2017.01.004.

99 M. Matusiak, S. Kadlubowski and P. Ulanski, Radiation-induced synthesis of poly(acrylic acid) nanogels, *Radiat.*

© 2024 The Author(s). Published by the Royal Society of Chemistry

Phys. Chem., 2018, **142**, 125–129, DOI: 10.1016/J.RADPHYSCHEM.2017.01.037.

100 A. Cruz, L. García-Uriostegui, A. Ortega, T. Isoshima and G. Burillo, Radiation grafting of *N*-vinylcaprolactam onto nano and macrogels of chitosan: Synthesis and characterization, *Carbohydr. Polym.*, 2017, **155**, 303–312, DOI: 10.1016/J.CARBPOL.2016.08.083.

101 M. Shahid, Z. H. Farooqi, R. Begum, M. Arif, A. Irfan and M. Azam, Extraction of cobalt ions from aqueous solution by microgels for *in situ* fabrication of cobalt nanoparticles to degrade toxic dyes: a two fold-environmental application, *Chem. Phys. Lett.*, 2020, **754**, 137645, DOI: 10.1016/j.cplett.2020.137645.

102 M. Arif, M. Shahid, A. Irfan, J. Nisar, X. Wang, N. Batool, M. Ali, Z. H. Farooqi and R. Begum, Extraction of copper ions from aqueous medium by microgel particles for *in situ* fabrication of copper nanoparticles to degrade toxic dyes, *Z. Phys. Chem.*, 2022, **236**(9), 1219–1241, DOI: 10.1515/zpch-2022-0038.

103 K. Naseem, R. Begum, W. Wu, M. Usman, A. Irfan, A. G. Al-Sehemi and Z. H. Farooqi, Adsorptive removal of heavy metal ions using polystyrene-poly(*N*-isopropylmethacrylamide-acrylic acid) core/shell gel particles: adsorption isotherms and kinetic study, *J. Mol. Liq.*, 2019, **277**, 522–531, DOI: 10.1016/j.molliq.2018.12.054.

104 R. G. Joshi, D. K. Gupta, P. Amesh, P. K. Parida and T. R. Ravindran, Microgel-hydrogel composite photonic crystals to monitor and extract uranyl ions in aqueous solutions, *Microporous Mesoporous Mater.*, 2021, **319**, 111075, DOI: 10.1016/J.MICROMESO.2021.111075.

105 F. Camerin, M. Á. Fernández-Rodríguez, L. Rovigatti, M. N. Antonopoulou, N. Gnan, A. Ninarello, L. Isa and E. Zaccarelli, Microgels Adsorbed at Liquid-Liquid Interfaces: A Joint Numerical and Experimental Study, *ACS Nano*, 2019, **13**, 4548–4559, DOI: 10.1021/ACSNANO.9B00390/ASSET/IMAGES/MEDIUM/NN-2019-003905_M152.GIF.

106 S. Ghasemi, M. Owrang and F. Javaheri, Kinetic and Equilibrium Function and Switchable Catalytic Activity of Some Thermo-Responsive Hydrogel Metal Absorbents Based on Modified PNIPAM, *J. Polym. Environ.*, 2023, **31**, 4972–4989, DOI: 10.1007/S10924-023-02915-W/FIGURES/14.

107 T. Kyrey, J. Witte, V. Pipich, A. Feoktystov, A. Koutsioubas, E. Vezhlev, H. Frielinghaus, R. von Klitzing, S. Wellert and O. Holderer, Influence of the cross-linker content on adsorbed functionalised microgel coatings, *Polymer*, 2019, **169**, 29–35, DOI: 10.1016/j.polymer.2019.02.037.

108 M. Arif, A review on advanced research of combine life of polystyrene (hard) and organic polymer (soft) materials: from 2018 to present, *Z. Phys. Chem.*, 2023, **237**, 809–843, DOI: 10.1515/ZPCH-2022-0142/MACHINEREADABLECITATION/RIS.

109 H. P. Ngang, A. L. Ahmad, S. C. Low and B. S. Ooi, Adsorption-desorption study of oil emulsion towards thermo-responsive PVDF/SiO_2-PNIPAM composite membrane, *J. Environ. Chem. Eng.*, 2017, **5**, 4471–4482, DOI: 10.1016/J.JECE.2017.08.038.

110 A. S. Al-Hussaini, K. M. Ossoss and M. E. R. Hassan, One-pot synthesis, characterization, and evaluation of novel Fe2O3@PANI-AA-o-PDA core-shell nanocomposites, *Polym.-Plast. Technol. Mater.*, 2021, **60**, 1331–1343, DOI: 10.1080/25740881.2021.1888994.

111 E. Wi, S. Go, S. Y. Shin, H. J. Cheon, G. Jeong, H. Cheon, J. Kim, H. R. Jung, H. Kim and M. Chang, Highly efficient and selective removal of anionic dyes from aqueous solutions using magneto-responsive Fe-aminoclay/Fe_2O_3/polyvinyl alcohol composite microgels, *Chem. Eng. J.*, 2023, **454**, 140309, DOI: 10.1016/J.CEJ.2022.140309.

112 K. Naseem, R. Begum, W. Wu, M. Usman, A. Irfan, A. G. Al-Sehemi and Z. H. Farooqi, Adsorptive removal of heavy metal ions using polystyrene-poly(*N*-isopropylmethacrylamide-acrylic acid) core/shell gel particles: adsorption isotherms and kinetic study, *J. Mol. Liq.*, 2019, **277**, 522–531, DOI: 10.1016/j.molliq.2018.12.054.

113 Z. Zhao, X. Zou, Y. Zhao, J. Shi, Y. Huang and J. Wang, Magnetic ion-imprinted microspheres for the removal of heavy metal ions from aqueous solution, *Environ. Prog. Sustainable Energy*, 2023, **42**, e13985, DOI: 10.1002/EP.13985.

114 N.-H. Cao-Luu, Q.-T. Pham, Z.-H. Yao, F.-M. Wang and C.-S. Chern, Synthesis and characterization of poly(N-isopropylacrylamide-co-acrylamide) mesoglobule core–silica shell nanoparticles, *J. Colloid Interface Sci.*, 2019, **536**, 536–547, DOI: 10.1016/j.jcis.2018.10.091.

115 N. H. Cao-Luu, Q. T. Pham, Z. H. Yao, F. M. Wang and C. S. Chern, Synthesis and characterization of PNIPAM microgel core–silica shell particles, *J. Mater. Sci.*, 2019, **54**, 7503–7516, DOI: 10.1007/S10853-019-03317-X/FIGURES/11.

116 Y. Y. Chuang, J. R. Deka, W. Y. Hsieh, S. P. Rwei, J. W. Shiu and T. F. Way, Synthesis and characterization of PNM@IAM core–shell microgels through inverse emulsion polymerization and its application for heavy metal ions capture, *J. Macromol. Sci., Part A: Pure Appl.Chem.*, 2023, **60**, 427–441, DOI: 10.1080/10601325.2023.2213699.

117 R. Mlih, J. Suazo-Hernández, Y. Liang, E. Tombácz, R. Bol and E. Klumpp, Polyacrylic-Co-Maleic-Acid-Coated Magnetite Nanoparticles for Enhanced Removal of Heavy Metals from Aqueous Solutions, *Colloids Interfaces*, 2023, **7**, 5, DOI: 10.3390/COLLOIDS7010005/S1.

118 L. Jiang, F. Chai and Q. Chen, Soft magnetic nanocomposite microgels by in-situ crosslinking of poly acrylic acid onto superparamagnetic magnetite nanoparticles and their applications for the removal of Pb(II) ion, *Eur. Polym. J.*, 2017, **89**, 468–481, DOI: 10.1016/J.EURPOLYMJ.2017.02.045.

119 M. Arif, Z. H. Farooqi, A. Irfan and R. Begum, Gold nanoparticles and polymer microgels: last five years of their happy and successful marriage, *J. Mol. Liq.*, 2021, **336**, 116270, DOI: 10.1016/j.molliq.2021.116270.

© 2024 The Author(s). Published by the Royal Society of Chemistry

120 M. Arif, A review on copper nanoparticles loaded in smart microgels, *Mater. Today Commun.*, 2023, **36**, 106580, DOI: 10.1016/j.mtcomm.2023.106580.

121 M. Arif, A Critical Review of Palladium Nanoparticles Decorated in Smart Microgels, *Polymers*, 2023, **15**, 3600, DOI: 10.3390/POLYM15173600.

122 X. Zhang, S. Xiong, C.-X. Liu, L. Shen, S.-L. Wang, W.-Z. Lang and Y. Wang, Smart TFC membrane for simulated textile wastewater concentration at elevated temperature enabled by thermal-responsive microgels, *Desalination*, 2021, **500**, 114870, DOI: 10.1016/j.desal.2020.114870.

123 T. Kureha, T. Shibamoto, S. Matsui, T. Sato and D. Suzuki, Investigation of changes in the microscopic structure of anionic poly(*N*-isopropylacrylamide-*co*-acrylic acid) microgels in the presence of cationic organic dyes toward precisely controlled uptake/release of low-molecular-weight chemical compound, *Langmuir*, 2016, **32**, 4575–4585, DOI: 10.1021/ACS.LANGMUIR.6B00760/SUPPL_FILE/LA6B00760_SI_002.PDF.

124 S. Backes, P. Krause, W. Tabaka, M. U. Witt, D. Mukherji, K. Kremer and R. Von Klitzing, Poly(*N*-isopropylacrylamide) Microgels under Alcoholic Intoxication: When a LCST Polymer Shows Swelling with Increasing Temperature, *ACS Macro Lett.*, 2017, **6**, 1042–1046, DOI: 10.1021/ACSMACROLETT.7B00557/SUPPL_FILE/MZ7B00557_SI_001.PDF.

125 A. M. Atta, A. K. Gafer, H. A. Al-Lohedan, M. M. S. Abdullah and A. O. Ezzat, Preparation of magnetite and silver poly(2-acrylamido-2-methyl propane sulfonic acid-co-acrylamide) nanocomposites for adsorption and catalytic degradation of methylene blue water pollutant, *Polym. Int.*, 2019, **68**, 1164–1177, DOI: 10.1002/PI.5809.

126 K. Sun, Y. Hu, Y. Dong, L. Yao, R. Song and Y. Xu, Tribological behavior of thermal- and pH-sensitive microgels under steel/CoCrMo alloy contacts, *Friction*, 2023, **11**, 602–616, DOI: 10.1007/S40544-022-0623-8/METRICS.

127 S. Alfei, F. Grasso, V. Orlandi, E. Russo, R. Boggia and G. Zuccari, Cationic Polystyrene-Based Hydrogels as Efficient Adsorbents to Remove Methyl Orange and Fluorescein Dye Pollutants from Industrial Wastewater, *Int. J. Mol. Sci.*, 2023, **24**, 1–33, DOI: 10.3390/ijms24032948.

128 S. Chen, X. Zhang, H. Huang, M. Zhang, C. Nie, T. Lu, W. Zhao and C. Zhao, Core@shell poly (acrylic acid) microgels/polyethersulfone beads for dye uptake from wastewater, *J. Environ. Chem. Eng.*, 2017, **5**, 1732–1743, DOI: 10.1016/J.JECE.2017.03.013.

129 D. Truzzolillo, S. Sennato, S. Sarti, S. Casciardi, C. Bazzoni and F. Bordi, Overcharging and reentrant condensation of thermoresponsive ionic microgels, *Soft Matter*, 2018, **14**, 4110–4125, DOI: 10.1039/C7SM02357J.

130 M. Arif, U. Fatima, A. Rauf, Z. H. Farooqi, M. Javed, M. Faizan and S. Zaman, A New 2D Metal–Organic Framework for Photocatalytic Degradation of Organic Dyes in Water, *Catalysts*, 2023, **13**, 231, DOI: 10.3390/CATAL13020231.

131 M. Arif, A Tutorial Review on Composites of Silica and Smart Microgels, *JOM*, 2024, **76**, 1203–1222, DOI: 10.1007/s11837-023-06294-4.

132 M. Arif, H. Raza, S. M. Haroon, K. Naseem, H. Majeed, F. Tahir, U. Fatima, S. M. Ibrahim and S. Ul Mahmood, Copper (II) ions extraction by poly(*N*-vinylcaprolactam-mathacrylic acid) microgels for *in situ* reduction formation of copper nanoparticles to reduce pollutants, *J. Mol. Liq.*, 2023, **392**, 123541, DOI: 10.1016/J.MOLLIQ.2023.123541.

133 K. Naseem, Z. H. Farooqi, R. Begum, M. Z. Ur Rehman, M. Ghufran, W. Wu, J. Najeeb and A. Irfan, Synthesis and characterization of poly(*N*-isopropylmethacrylamide-acrylic acid) smart polymer microgels for adsorptive extraction of copper(II) and cobalt(II) from aqueous medium: kinetic and thermodynamic aspects, *Environ. Sci. Pollut. Res.*, 2020, **27**, 28169–28182, DOI: 10.1007/S11356-020-09145-W/TABLES/4.

134 J. Yun, Y. Wang, Z. Liu, Y. Li, H. Yang and Z. Xu, High efficient dye removal with hydrolyzed ethanolamine-Polyacrylonitrile UF membrane: rejection of anionic dye and selective adsorption of cationic dye, *Chemosphere*, 2020, **259**, 127390, DOI: 10.1016/j.chemosphere.2020.127390.

135 W. Guan, C. Lei, Y. Guo, W. Shi and G. Yu, Hygroscopic-Microgels-Enabled Rapid Water Extraction from Arid Air, *Adv. Mater.*, 2022, 2207786, DOI: 10.1002/adma.202207786.

136 S. Backes, P. Krause, W. Tabaka, M. U. Witt and R. Von Klitzing, Combined Cononsolvency and Temperature Effects on Adsorbed PNIPAM Microgels, *Langmuir*, 2017, **33**, 14269–14277, DOI: 10.1021/ACS.LANGMUIR.7B02903/ASSET/IMAGES/MEDIUM/LA-2017-02903S_0007.GIF.

137 L. Xia, Q. Cui, X. Suo, Y. Li, X. Cui, Q. Yang, J. Xu, Y. Yang and H. Xing, Efficient, Selective, and Reversible SO2 Capture with Highly Crosslinked Ionic Microgels *via* a Selective Swelling Mechanism, *Adv. Funct. Mater.*, 2018, **28**, 1704292, DOI: 10.1002/ADFM.201704292.

138 Z. Guo, Q. Chen, H. Gu, Z. He, W. Xu, J. Zhang, Y. Liu, L. Xiong, L. Zheng and Y. Feng, Giant Microgels with CO_2-Induced On–Off, Selective, and Recyclable Adsorption for Anionic Dyes, *ACS Appl. Mater. Interfaces*, 2018, **10**, 38073–38083, DOI: 10.1021/ACSAMI.8B13448/SUPPL_FILE/AM8B13448_SI_002.AVI.

139 Y. Yang, X. Xu, Y. Guo and C. D. Wood, Enhancing the CO_2 capture efficiency of amines by microgel particles, *Int. J. Greenh. Gas Control*, 2020, **103**, 103172, DOI: 10.1016/j.ijggc.2020.103172.

140 F. Wang, Z. Liu, R. Xie, X.-J. Ju, W. Wang, D.-W. Pan and L.-Y. Chu, Poly(N-isopropylmethacrylamide-co-4-acrylamidobenzo-18-crown-6) microgels with expanded networks for excellent adsorption of lead(II) ions, *Particuology*, 2023, **77**, 105–115, DOI: 10.1016/j.partic.2022.09.002.

141 N. Allahyar and C. Özeroğlu, Kinetics and equilibrium study of the adsorption of silver ions by polymeric composites containing zeolite and methacrylic acid, *J.*

© 2024 The Author(s). Published by the Royal Society of Chemistry

Iran. Chem. Soc., 2022, **19**, 1689–1700, DOI: **10.1007/S13738-021-02410-W/FIGURES/15**.

142 J. Zhang, L. Mei, N. Chen, Y. Yuan, Q. Z. Zeng and Q. Wang, Study on β-lactoglobulin microgels adsorption onto a hydrophobic solid surface by QCM-D, *Food Hydrocolloids*, 2020, **98**, 105320, DOI: **10.1016/J.FOODHYD.2019.105320**.

143 J. Yao, H. Yang, D. Zuo, J. Xu and H. Zhang, Facile Preparation and Adsorption Behavior Studies of Poly(acrylic acid)-Based Hydrogels Reinforced by Hydrogen Bonds for Methylene Blue Dye, *J. Polym. Environ.*, 2023, **31**, 552–564, DOI: **10.1007/s10924-022-02610-2**.

144 B. Pany, A. Ghosh Majundar, M. Mohanty, K. P. Fyis, T. Dey, G. Tripathy, S. Bhat, J. Yamanaka and P. S. Mohanty, Polymerized stimulus–responsive microgels for the removal of organic dye from water, *J. Mol. Liq.*, 2023, **375**, 121267, DOI: **10.1016/j.molliq.2023.121267**.

145 M. Chen, K. R. Kumrić, C. Thacker, R. Prodanović, G. Bolognesi and G. T. Vladisavljević, Selective Adsorption of Ionic Species Using Macroporous Monodispersed Polyethylene Glycol Diacrylate/Acrylic Acid Microgels with Tunable Negative Charge, *Gels*, 2023, **9**, 849, DOI: **10.3390/GELS9110849**.

146 S. T. Maleki, P. Beigi and M. Babamoradi, Synthesis of pectin hydrogel/Fe3O4/Bentonite and its use for the adsorption of Pb (II), Cu (II), and Cd (II) heavy metals from aqueous solutions, *Mater. Sci. Eng. B*, 2023, **298**, 116899, DOI: **10.1016/J.MSEB.2023.116899**.

147 S. Xu, D. Li, Y. Zhu, J. Guo, Y. Ai, Q. Chu, X. Yun, X. Li and L. Wang, Multilayer films of graphene oxide and polymeric microgels: reusable adsorbents, *Aust. J. Chem.*, 2023, **76**, 600–614, DOI: **10.1071/CH23068**.

148 M. C. Tatry, E. Laurichesse, A. Perro, V. Ravaine and V. Schmitt, Kinetics of spontaneous microgels adsorption and stabilization of emulsions produced using microfluidics, *J. Colloid Interface Sci.*, 2019, **548**, 1–11, DOI: **10.1016/J.JCIS.2019.04.020**.

149 X. C. Weng, M. Ajmal, H. Shehzad, J. Chen, Z. H. Farooqi, Z. Liu, A. Sharif, E. Ahmed, L. Zhou, L. Xu, J. Ouyang, A. Irfan, A. R. Chaudhry, R. Begum and S. Shaukat, Tungsten oxide encapsulated phosphate-rich porous alginate composites for efficient U(VI) capture: Insights into synthesis, adsorption kinetics and thermodynamics, *Int. J. Biol. Macromol.*, 2024, **261**, 129962, DOI: **10.1016/J.IJBIOMAC.2024.129962**.

© 2024 The Author(s). Published by the Royal Society of Chemistry